

Modified Surfaces with Nano-Structured Composites of Prussian Blue and Dendrimers. New Materials for Advanced Electrochemical Applications

Erika Bustos* and Luis A. Godínez

Centro de Investigación y Desarrollo Tecnológico en Electroquímica, S. C. Parque Tecnológico Querétaro, Sanfandila, Pedro Escobedo, 76703, Querétaro.

*E-mail: ebustos@cideteq.mx

Received: 11 November 2010 / Accepted: 1 December 2010 / Published: 1 January 2011

In this work, the basic theory and the applications of modified surfaces with nano-structured composites of Prussian Blue (PB) and Dendrimers, for the electrochemical detectors and electro-catalyze technologies, currently, represent some of the most promising approaches for the development of efficient and new materials for advanced electrochemical applications. As the PB interacts in supramolecular manner with PAMAM dendrimers in aqueous medium, across the hydrophobic zone of dendrimer, they form composites stables in solution with different generations of PAMAM. Dendrimers make the function of endoreceptors of PB forming composites of PB – PAMAM dendrimers, which can be used to construct PB films over gold surfaces, in covalent or electrostatic modification process, which can work as electro-catalysers to detect molecules with biological importance.

Keywords: Composites, prussian blue, dendrimers.

1. INTRODUCTION

The new construction of composites is necessary to elevate different physicochemical properties of novel surfaces. This is the case of modified surfaces with nano-structured composites of Prussian Blue (PB) and Dendrimers to be applied as electrochemical detectors and electro-catalyze technologies.

In this sense, this paper shows in the first part the general properties of PB and PAMAM dendrimers, to understand their interaction and stability in solution. The second part of the paper shows the construction of PB – PAMAM composites and the different analytical techniques to thier

characterization. The next part of the paper, it shows the construction of the new modified electrodes with electrochemical and electrocatalytic properties. Finally, the paper describes the application of the modified electrodes with these composites in the detection of molecules with biological importance as dopamine and hydrogen peroxide.

2. PHYSICOCHEMICAL CHARACTERISTICS OF PRUSSIAN BLUE AND PAMAM DENDRIMERS

Solid metal hexacyanometalates of the type $(M^+)_{n}M'[M''(CN)_6]$, where M' and M'' denote transition metals (i. e. Fe^{2+}/Fe^{3+} , Ni^{2+}/Ni^{3+} or Cu^{2+}/Cu^{3+}), are very useful as ion – selective materials, because the redox reaction of lattice metal ions are accompanied by a reversible exchange of cations between the electrolyte solution and interstitial holes of the solid compound, across them there is a diffusional transference of contraions which gives to prussian compounds the solubility in aqueous media [1-2].

2.1. Prussian Blue.

Two stoichiometries have been reported for the chemically prepared PB film, namely the insoluble form $Fe_4[Fe(CN)_6]_3 \cdot 6H_2O$ and the soluble form $KFeFe(CN)_6$. The redox reaction of the soluble form is [3]:



And that of the insoluble form is [4]:



PB, $KFe^{III}[Fe^{II}(CN)_6]$, is a prototype of metal hexacyanoferrates. It is used commonly as a model redox –active solid for both fundamental and applied studies.

From a structural viewpoint, PB form a rigid three-dimensional cubic network of repeating –NC-Fe-CN-M-CN units (Figure 1) [5-6].

The first structural hypothesis by the PB, it was derivate from X-Ray powder patterns and postulated the occurrence of interstitial metal ions within the cubic face-centered unit cell in order to achieve electroneutrality. According to this model, the unit cell contains 4/3 formula units of $Fe_4[Fe(CN)_6]_3$, i. e., 4 ferrocyanide octahedral (Fe in “C hole”), 4 iron (III) coordinated by the nitrogen end of the cyanide (“N hole”), and 4/3 ferric ions randomly distributed in an eightfold interstitial position [10-11].

PB has a face-centered-cubic structure in which Fe^{3+} is high spin with $S = 5/2$ and Fe^{2+} is low spin with $S = 0$. It shows a long-range ferromagnetic ordering at $T_c = 5.6K$ in which magnetic

interactions occur between the Fe³⁺ ions through the 10 Å long Fe³⁺ - NC - Fe²⁺ - CN - Fe³⁺ linkages, which is the value of the cell constant [5, 10, 12-16].

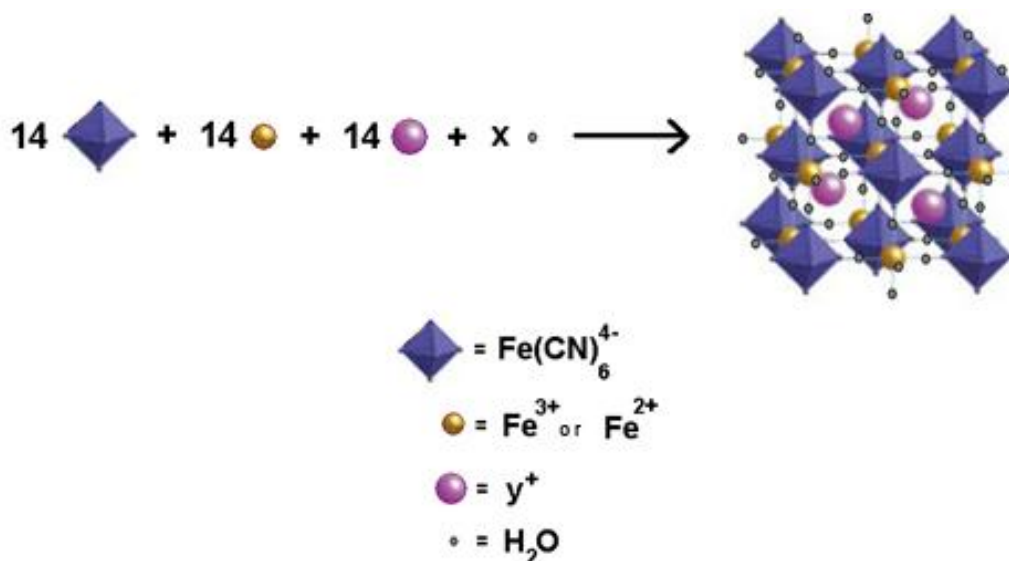


Figure 1. Schematic representation of the diffusion of potassium across the vacuum spaces of the structure of Fe^{III}[Fe^{II}(CN)₆] [7-9].

The synthesis of PB has been made with a mix of ferric salt (Fe^{III}) with ferrocyanide (Fe^{II}), ferrose salt (Fe^{II}) with ferricyanide (Fe^{III}), ferrose salt with ferrocyanide and an oxidation reaction, galvanostatic deposit of ferrocyanide at acid pH [17-18], and electrochemical deposit with cyclic scan of the oxidation of ferrocyanide in acid pH with KCl (Table 1) [7, 19], with the general reaction of:

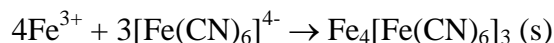
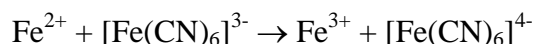


Table 1. Different methods of PB synthesis there are applied [20-25].

Solution	Method	Electrodes
Fe(CN) ₆ ³⁻ .	Adsorption.	Gold.
Fe(CN) ₆ ³⁻ + Fe ²⁺ .	Electrochemical cyclic.	Glassy Carbon.
Fe(CN) ₆ ³⁻ + Fe ³⁺ .	Galvanostatic Electrodeposit.	Black Carbon.
Fe(CN) ₆ ³⁻ + Fe(CN) ₆ ⁴⁻ .	Potenciostatic Electrodeposit.	ITO (In(SnO ₂)).
Fe(CN) ₆ ⁴⁻ .	Inmersion.	Platinum.
Fe(CN) ₆ ⁴⁻ + Fe ²⁺ .	Coloidal Solution.	SnO ₂ .
Fe(CN) ₆ ⁴⁻ + Fe ³⁺ .		

To synthesize PB is important to have the two oxidation states of iron, to be sure that electronic transferred will be present across the cyanide link. For example, in the case of mix potassium ferrocyanide ($K_2Fe(CN)_6$) with a ferrous salt ($FeCl_2$) in a buffer of phosphate pH 2, the Fe^{II} of ferrocyanide change to Fe^{III} (Figure 2-B), and the PB can be synthesized and showing the precipitate of PB with the time (Figure 2-C), as the next reaction shows:

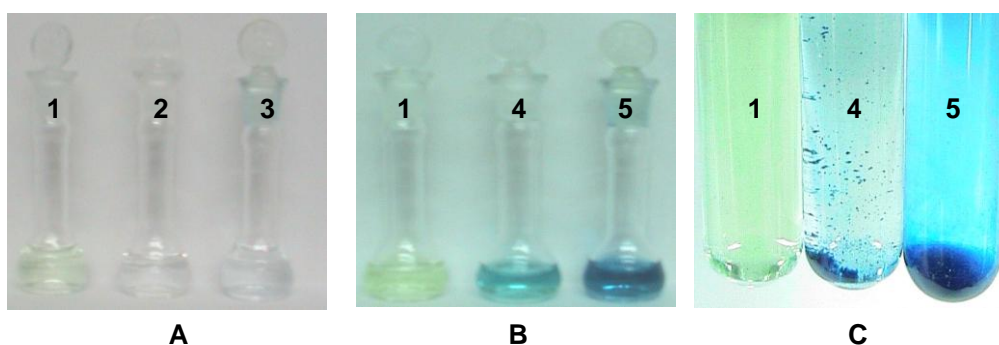
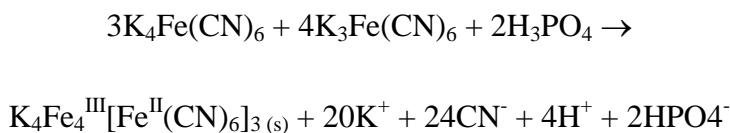


Figure 2. Synthesis of PB with $K_4Fe(CN)_6$ (1), $FeCl_2$ (2) and $FeCl_3$ (3) solutions in phosphate buffer pH 2 (A), with the mix of 1+2 (4) and 1+3 (5), at 0 min (B) and after 24 h with PB precipitated (C).

The studies of soluble and insoluble PB have been performed by many methods, as: X – ray diffraction [10-11], X – ray absorption fine structure spectroscopy (EXAFS) [26], oxidization potential, a paramagnetic susceptibility (Mössbauer study) and a phonon absorption spectrum [27].

With the aid of X-ray powder diffraction, they discovered that there were two different structures for PB, called insoluble PB ($Fe_4[Fe(CN)_6]_3$) (Figure 3) and soluble PB ($KFeFe(CN)_6$). The difference between insoluble and soluble PB results from the degree of peptization to potassium salts. Both are nearly insoluble in water. It is easy for soluble PB to undergo peptization with potassium salts in solutions, so they are called “soluble” by dying industrialists. These compounds have a 3D structure similar to the crosslinking in polymers, thus they can be easily combined with solvents and their stoichiometric number may change [28].

For insoluble PB, ferric ions occupy the cell interstitial sites. In soluble PB, the structure is basically the same except that potassium ions replace some of the ferric ions in the interstitial sites. PB acts like a zeolite and the diameter of the channel formed by the lattices is about 3.2 \AA [28]. The size of the hydrated cations must be smaller than Stokes’ radii [24, 29-31] as K^+ , Rb^+ , Cs^+ , NH_4^+ , H^+ , inserting / extracting into and /or out of the PB lattice structure during the reduction of the high – spin

iron ions [4, 28, 32-33], while larger ions such as Na^+ , Li^+ , Mg^{2+} and Ca^{2+} are a group of cations which blocked, by the small channels in the lattice of PB [1-2, 28, 34].

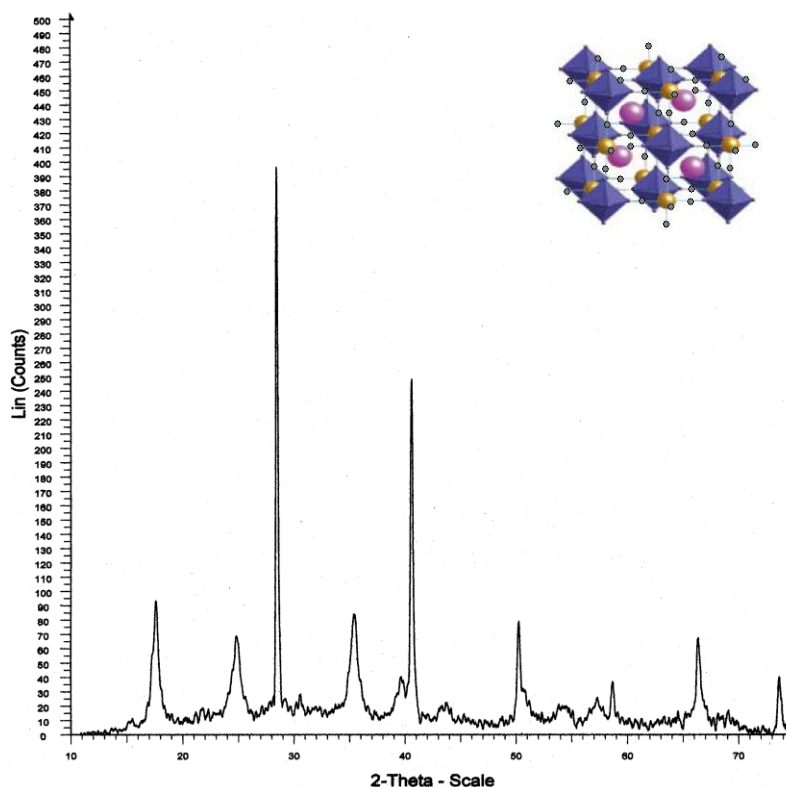


Figure 3. Diffractogram of PB synthesized with 0.1mM FeCl_3 and 0.1M $\text{K}_2\text{Fe}(\text{CN})_6$ in phosphate buffet pH 2, after one month of dried.

Considering that the PB reaction had been employed only in qualitative tests, a first experiment was made to obtain the UV- Visible absorption spectrum of this compound. Fe(III) mixed with hexacyanoferrate (III), and a strong absorption band can be observed in the UV region and a weaker band with wavelength peak at 420 nm, which is related to the formation of the brown complex hexacyanoferrate (III) ferric [20, 35].

By the physicochemical properties of PB, it is a prototype of metal hexacyanoferrate, and is well known for batteries in solid state [36-39], inhibitors of corrosion [36], paints [36], lacquers [36], inks [36], electrochromic surfaces [40-47], electrochemical catalysis [28, 48-50], photophysical [51-55], magnetic properties [14, 56-65], membranes of ionic interchange and analytical applications of ions [66-67] and compounds [48, 66, 68-78].

Comparing those of bulk materials with nanosized PB, large surface – to – volume ratio and the increased surface activity qualify its use in catalysis and sensing. Recently, several groups have reported the marvelous electrocatalytic character of inorganic Prussian Blue NanoParticles (PBNPs) towards the electro-oxidation or electro-reduction compared with that of the conventional PB

microparticles or polycrystalline film. This kind of materials have high sensitivity and specificity thus eliminating problems with interfering compounds [69, 80].

In this manner, several studies have showed the electrocatalytic effects that Prussian Blue (PB, $\text{Fe}_4[\text{Fe}(\text{CN})_6]_3 \cdot \text{H}_2\text{O}$) films confined on an electrode surface have on the potassium [81-82], cesium [83], thallium, ammonium [84], rubidium [85] and other cations [86]. In addition, O_2 [28, 87], hydrazine [87], glucose [73, 79, 88-90], ascorbic acid [70, 91] H_2O_2 [28, 79, 80-92], arsenite (AsO_2^- , As^{3+}) [93], persulfate ($\text{S}_2\text{O}_8^{2-}$) [94] electrochemical reactions have been evaluated in presence of PB.

2.2. PAMAM Dendrimers.

Polyamidoamine (PAMAM) dendrimers are known as cascade polymers, arborols, or hyper-ramified polymers, are a relatively new class of materials [95-97]. Dendrimer molecules can be basically described as the result of the sequential modification of a polyfunctional core with multifunctional monomers, also called dendrons. These monomeric units are designed in such a way that, after each growing step, while the radius of the polymer is increased in a linear fashion, the number of terminal groups in the polymer grows in a geometric way as a consequence of the hyper-ramified nature of the dendrons, increasing the generation of dendrimer. The generation depends of the number of terminal functional groups and the size of diameter of dendrimer (Figure 4) [98].

Dendrimer molecules possess three basic architectural components: an initiator core (e.g., ethylenediamine), interior layers often called “generations”, which compose repeating units attached to the initiator core, and the shell which generally consists of functionalized groups attached to the outermost interior layer. Dendrimers of lower generations tend to exist in relatively open forms, while high generation dendrimers take on a spherical three-dimensional structure (Figure 4) [99].

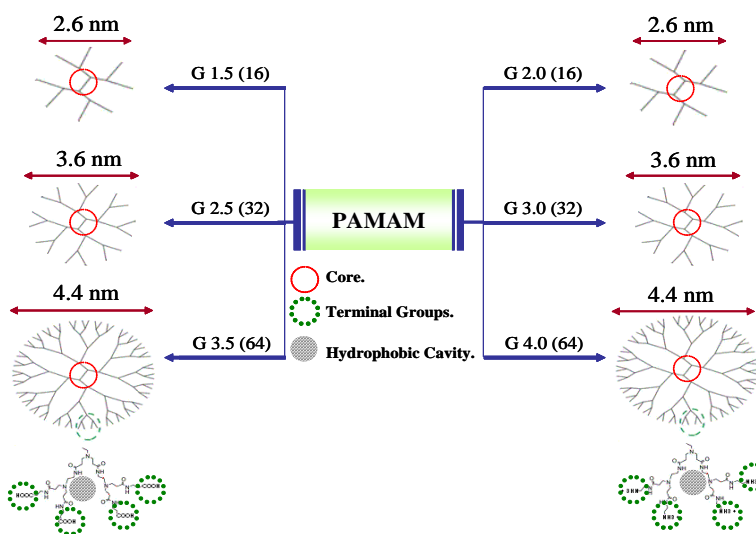


Figure 4. Representation of different generation (G) of PAMAM dendrimer with carboxylic (G1.5, G2.5 and G3.5) and amine terminal (G2.0, G3.0, G4.0), indicating the core, terminal groups and hydrophobic cavity of dendrons. Between parenthesis is the size of dendrimer in nanometers, in order of each generation.

Dendrimer – Encapsulated Nanoparticles (DENs) are prepared by a two – step process [110]. First, metal ions are extracted into dendrimers where they coordinate in fixed stoichiometries with interior functional groups. Second, the metal – ion / dendrimer composites are reduced to yield encapsulated nanoparticles. This process leads to stable nearly size – monodisperse, catalytically active nanoparticles composed of Pt [111-114], Pd [105, 112-116], Au [117-120] or Cu [121]. It is possible to prepare alloy [122-124] and core/shell [123-124] bimetallic nanoparticles using a slight variation on this basic synthetic scheme (Figure 5).

Hybrid nanoparticles of carboxyl-terminated PAMAM dendrimers containing encapsulated Pt nanocrystals were prepared, and reports on the fabrication of Au, Cu, and Pd nanoparticles within PAMAM dendrimer have also been made [125-126].

An advantage of PAMAM nanoreactors is the small nanoparticles diameter. Metal nanoparticles (less than 4 nm in diameter) are interesting because of their inherent size – dependent optical, electrical, catalytic, and magnetic properties [99, 127]. These materials have been integrated into new kinds of biosensors, have shown effects of particle size on heterogeneous catalytic reactions, and have been used for the fabrication of nanometer-scale electronic devices, supercapacitors, and data storage devices [99, 126-129].

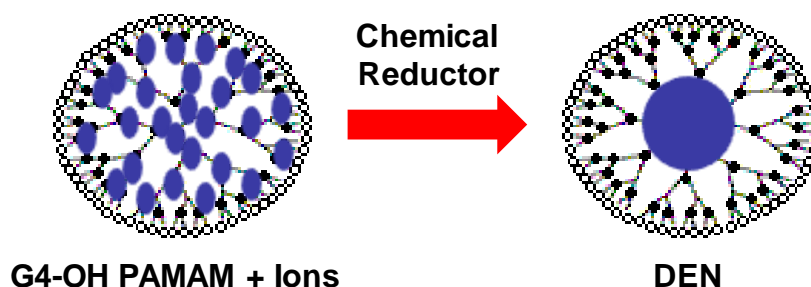


Figure 5. Schematic representation of PAMAM dendrimer encapsulates metallic ions, which they were reduced chemically to form the nanoparticles.

3. NANO-STRUCTURED COMPOSITES OF PRUSSIAN BLUE AND DENDRIMERS.

The synthesis and application of PB nanoparticles have demonstrated an extremely promising prospect since the nanostructures often exhibit novel size – dependent properties that cannot be achieved by their bulk form, and give rise to porous, high – surface area electrodes, where the local microenvironment can be controlled by the crosslinking elements and may lead to specific and selective interactions with substrates.

In this sense, the PB nanoparticles can be introduced in the hydrophobic interior of PAMAM to synthesized composites PB – PAMAM dendrimers. This kind of material results in a novel electrocatalytic and stable compound which can be used in neutral conditions without precipitation of PB, which results in a new compound that can be characterized with spectroscopical techniques.

3.1. Synthesis of the Composites PB – PAMAM dendrimers.

The reported methods include doping carbon inks or paste with PB powder, adsorption of PB – polymer (polyethyleneimine –PEI- [130]), the encapsulation of metal hexacyanoferrates in sol – gel matrices [131], composite with gold nanoparticles, combination of PB nanoparticles and Multi-Walled Carbon NanoTubes (MWCNTs) in the matrix of biopolymer chitosan [68, 78] and dendrimer – supported PB synthesis (Figure 6) [99, 107-109, 132].

The PB with the time precipitates in acid conditions (Figure 7 - A), but in presence of 50 μ M PAMAM G3.5 (Figure 7 - B) or G4.0 (Figure 7 - C), the precipitate does not appear even after 2 days, suggesting an interaction between the dendrimer molecules and the PB species that prevents the precipitate from appearing.

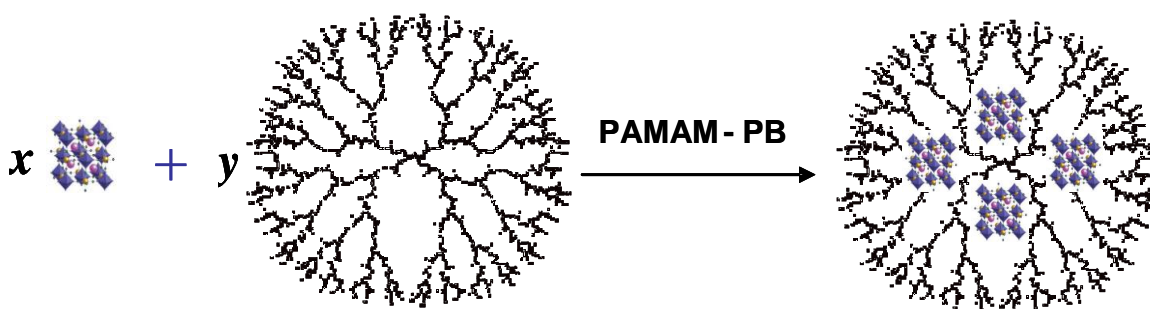


Figure 6. Representation the endoreception of PB in the PAMAM G4.0., with 64 terminal amines.

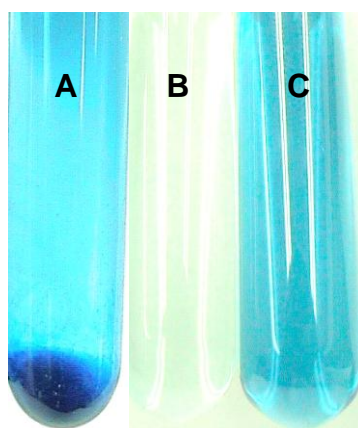


Figure 7. Images of PB synthesized with 1mM FeCl₃ + 1mM K₄Fe(CN)₆ in phosphate buffered aqueous solution pH 2 at 298 K (A), in the presence of 50 μ M PAMAM G3.5 (B) and 50 μ M PAMAM G4.0 (C).

3.2. Characterization of the Composites PB – PAMAM dendrimers.

A simple technique to characterize PB is with Ultraviolet Visible Spectroscopy (UV-Vis), because this compound is a chromophore with a solubility constant (K_s) of $3.0 \times 10^{-41} \text{ M}^{-1}$ [20, 133],

molar absorptivity (ϵ) of $3.0 \times 10^4 \text{ L mol}^{-1}$ [20] and its electronic transition between $\text{Fe}^{3+} - \text{C} - \text{N} - \text{Fe}^{2+}$ is around 700 nm (Figure 6) [1, 20, 22]. The figure 8 shows that dendrimers stabilized the PB in solution independent of the terminal groups of the dendrimer molecule, observing a similar absorption coefficients, which suggest that the interaction of the PB species and the two dendrimer molecules must take place within the polymeric PAMAM host.

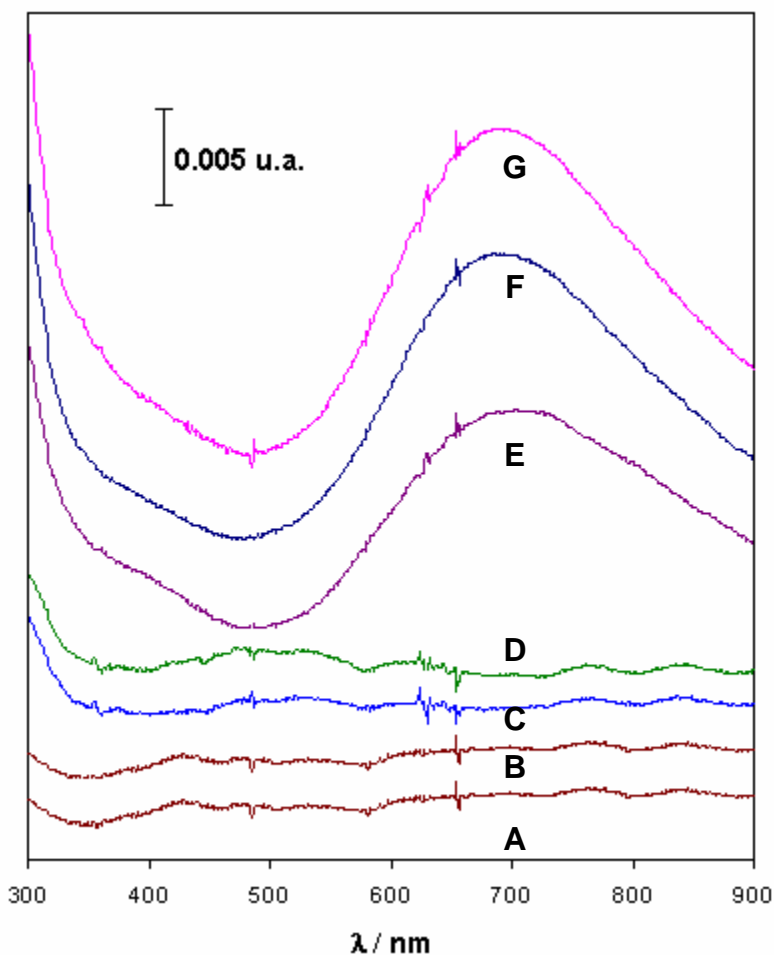


Figure 8. Ultraviolet-Visible spectrum of 50 μM FeCl_3 (A), 50 μM $\text{K}_4\text{Fe}(\text{CN})_6$ (B), 1 μM PAMAM G3.5 (C), 1 μM PAMAM G4.0 (D), 50 μM PB (E), 50 μM PB + 1 μM PAMAM G3.5 (F) and 50 μM PB + 1 μM PAMAM G4.0 (G) in phosphate buffered aqueous solution pH 2 at 298 K.

4. MODIFIED SURFACES WITH NANO-STRUCTURED COMPOSITES OF PRUSSIAN BLUE AND DENDRIMERS

The modified electrodes can be prepared from ferrocyanide ($\text{K}_4\text{Fe}(\text{CN})_6$) aqueous solutions in the presence of Fe^{3+} or Fe^{2+} salts over gold with, or without, previously attaching organic modifiers by means of adsorption and/or electrochemical techniques. The stability and activity of modified electrode

has been reported to be sensitive to several parameters among which, solution composition, pH (must be < 5), temperature and the nature of the counterion species (like K^+ , H^+ and NH_3^+).

Due to PB has low solubility in aqueous acid solutions, it has been successfully adsorbed on the surfaces of different electrode materials and it has been found to be a good electrocatalyst for several specific reactions. The main problem of the chemically modified electrodes reported to date, however, relies on the fact that the electrocatalytic film of PB is stable only at low pH values ($pH < 5$) [1-2, 21, 48, 134], and therefore, its integrity and activity are seriously compromised by bulk and local changes in pH that offer appear as a consequence of electron –transfer events in the interphasial region [135].

PB thin films can be therefore synthesized over covalently or electrostatically modified gold substrates with PAMAM dendrimer, resulting novel substrates with novel properties such as hydrophobicity, mechanical and chemical stability, permeability and electrocatalytic activity towards reactions already catalysed by PB typical films, due to the combination of the relevant modifying molecules, improving in this way the sensitive as well as the selectivity of certain specific electrochemical reactions.

4.1. Design and Construction of Modified Surfaces with Composites PB – PAMAM dendrimers.

Films of PB have been deposited on various substrates such as platinum [21-22, 134-135], gold [22, 136-137], graphite [21-22, 134], glass vitreous carbon [21, 134], fiber of carbon [21], paste of carbon [21, 138], SnO_2 [22], $In(SnO_2)$ [22] and ITO, by simple immersion or adsorption, electrodeposition, and entrapping them in polymers [139]; also, chemical deposition of PB onto the surface of pretreated screen – printed carbon electrodes [80].

Even if actually there is no consensus on the best method to obtain high-quality deposits, the fact that the electrochemical response of the films is strongly dependent on their history and elaboration is uniformly adopted.

It has been shown, for example, that soluble PB films ($KFe[Fe(CN)_6]$), which are obtained from the initially formed insoluble PB deposits ($Fe_4[Fe(CN)_6]_3$) by successive cycling around the reduction system PB / Everitt's salt ($K_2Fe[Fe(CN)_6]$) in KCl aqueous solutions, are more stable than their precursors against cycling around the oxidation system PB / Prussian Yellow ($Fe[Fe(CN)_6]$) [22].

On other hand, pre-concentration methods at the electrode-solution interphase are available and work is currently being undertaken in order to increase the analytic sensitivity of amperometric detection protocols [140].

One interesting approach along these lines, consists on modifying electrodes with monolayers of polyamidoamine (PAMAM) dendrimers that can specifically interact with the molecules of interest.

The approach relies on the fact that dendrimers, being synthetic macromolecules which consist of a central core surrounded by alternating layers of branching units, are capable of forming thin and porous films that allow electron transfer processes to take place when adsorbed on electrode surfaces [107], as the case of cobalt hexacyanoferrate (Figure 9) [141-142].

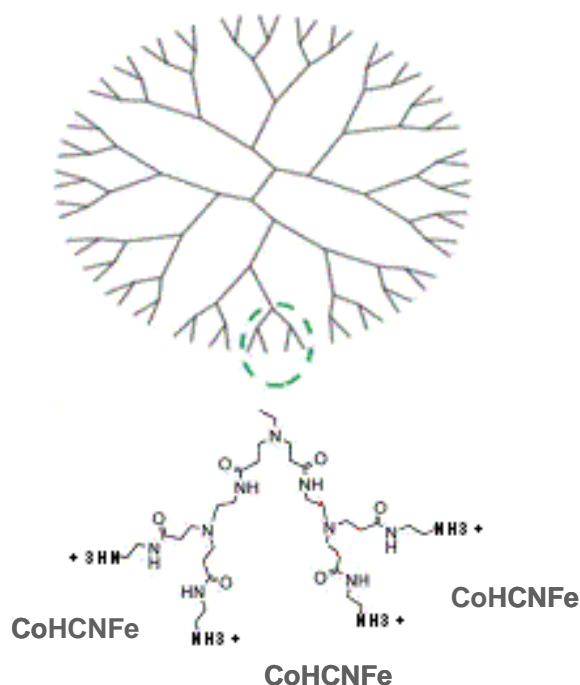


Figure 9. Schematic representation of the synthesis of gel with PAMAM dendrimer G4.0 and cobalt hexacyanoferrate (CoHCF).

In addition to their interesting electrode modification properties, PAMAM dendrimers can also be used to prepare and accommodate catalytic nano-sized metallic particles. These monodisperse metallic particle-dendrimer nano-composites, have been shown to efficiently catalyze specific reactions of alcohols [143] and oxygen [144], by conveniently eliminating aggregation and blocking of active sites on the surface of the metallic clusters, thus increasing the catalytic efficiency [145].

The quality of electrodes modify by Prussian Blue films can be judged by the sharpness of the oxidation and reduction peaks in cyclic voltammograms. To achieve a regular structure of the PB films, two main factors should be taken into account, namely, the electrodeposition potential and pH of the initial solution of iron salts.

The working electrode potential should not be lower than 0.2V because otherwise, reduction of ferricyanide ions takes place. The pH value of the initial solution optimal for film deposition is 1 [146-147].

Modified electrodes with nanocomposites of PAMAM dendrimers with inorganic nanoelectrocatalysts can be using gold electrodes [108] modified with covalent linkages through 3-mercaptopropionic acid (SH) and carbodiimide (EDC) to amine-terminated PAMAM dendrimers of several different generations (PG_x, x = 2.0, 3.0 or 4.0) and loaded with PB (Figure 10 - A). In the same manner, modified electrodes with PAMAM G1.5, G2.5 and G3.5 can be constructed using 2-aminoethanethiol (SH) and EDC [107-109]. In addition, the electrostatically modification of PAMAM – PB without the presence of thiols and chemical reductor (Figure 10 - B) [108]. Just now, only these kind of dendrimers are used to modified surfaces with PB by the amine and carboxylic terminal groups, which generate acid interface to solubilized and distribute in better manner the PB on surface.

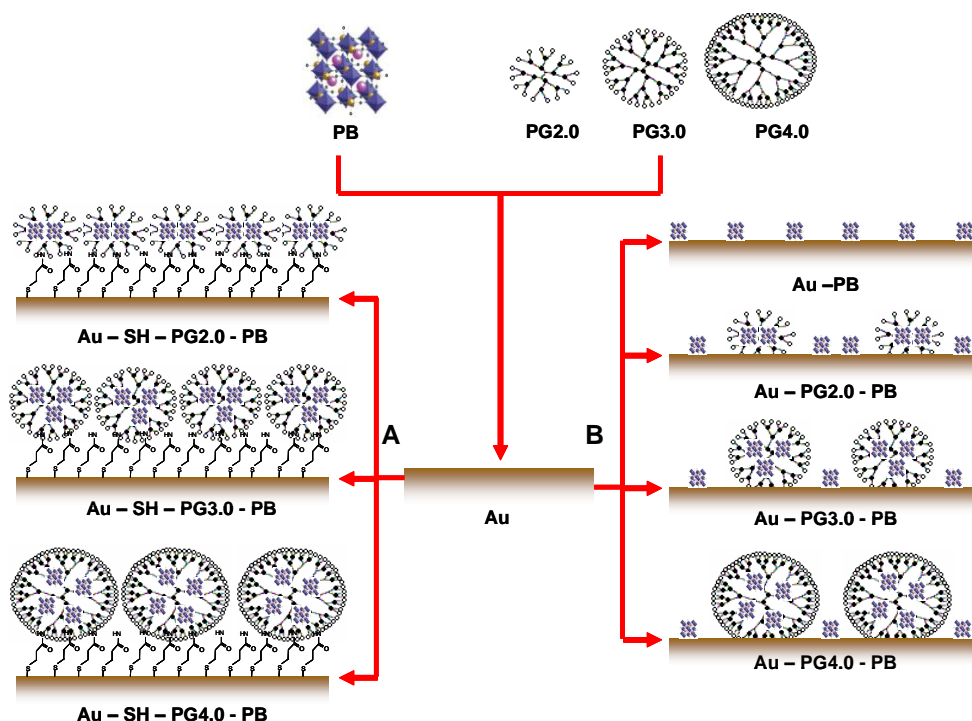


Figure 10. Schematic representation of the covalent (A, Au-SH-PG_x-PB with EDC) and electrostatically (B, Au-PG_x-PB without SH and EDC) modification methodology.

As represented by Figure 10-A, the test group of Au-bead electrodes were exposed to 1mM 3-mercaptopropionic acid or 2-aminoethanethiol (SH) in methanol for 12 h, attaining a thiol coverage of $\cong 1.60 \times 10^{-10} \text{ mol cm}^{-2}$ and $2.05 \times 10^{-10} \text{ mol cm}^{-2}$, respectively [107]. Such coverage indicates that the chemically adsorbed thiols form a submonolayer over 20 % of the electrode surface [107]. Next, the thioled surfaces were modified by adsorption of PAMAM dendrimers of a specific generation from a 50 μM solution in methanol forming typical self-assembling sub-monolayers through peptidic bonds, which were generated by the assistance of 10 mM EDC in the dendrimer containing solution. PB is incorporated on the modified electrode surfaces by placing the electrodes in acidic aqueous phosphate-buffered solution (pH 2, I=0.1) containing equimolar quantities (1.0 mM) of FeCl_3 and $\text{K}_4\text{Fe}(\text{CN})_6 \cdot 3\text{H}_2\text{O}$ for 12 h at 298 K under a N_2 atmosphere [107]. This treatment produced electrodes designated as: Au – SH – PG2.0 – PB, Au – SH – PG3.0 – PB and Au – SH – PG4.0 – PB, according to the generation of dendrimer present.

On other hand, bare gold electrodes were electrostatically modified directly without thiol by exposure to solution of PAMAM dendrimer of a specific generation (50 μM) containing 1mM PB, in pH 2 phosphate buffer for 12 h at 298K under N_2 atmosphere. In this manner, three physically modified electrodes were produced and designated as: Au – PG2.0 – PB, Au – PG3.0 – PB and Au – PG4.0 – PB (Figure 10 - B).

A similar manner modified surfaces with PAMAM / nano – Au / PB films anchored on 3-mercaptopropionic acid (MPA) – modified electrode was reported [135, 148] to be used to electrocatalytic activity (SH) of H_2O_2 . In this case, the Au / MPA / PAMAM membrane electrode was transferred into gold colloid solution for 12 h at 4°C to obtain Au / SH / PAMAM / nano – Au

modified electrodes. PB was electrodeposited immersing the pre-processed electrode in a carefully deoxygenated (20 min) solution containing 2.5 mM FeCl_3 , 2.5 mM $\text{K}_3\text{Fe}(\text{CN})_6$, 0.1M KCl and 0.1M HCl, followed by a cyclic scan in a potential range of -0.5 to +0.65V at 50 mVs^{-1} for 15 cycles. After deposition, the electrodes were thoroughly washed with double – distilled water, then transferred into a supporting electrolyte solution (0.1 M KCl + 0.1M HCl) and electrochemically activated by cycling between +350 and -50 mV (25 cycles) at a rate of 50 mVs^{-1} . Finally the electrodes were taken out and rinsed with double – distilled water again. Like gold nanoparticles were over the surface of the PAMAM dendrimers, the PB was developed over the nano-Au, as figure 11 shows. On the nano-Au-modified electrode surface was completely coated by a homogeneous and compact agglomerates PB grains compared with the particle size of PB is smaller.

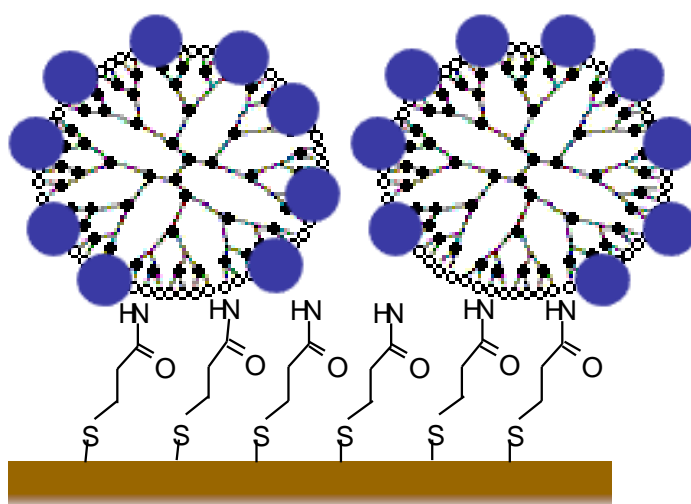


Figure 11. Schematic representation of the synthesis of Au / MPA / PAMAM / nano – Au / PB.

On other way, using as precursor of increase the PB in the interface of modified electrode, it was the fabrication of nanostructured films comprising nanoparticles – containing amine – terminated G4 PAMAM dendrimer and poly (vinylsulfonic acid) (PVS) through the layer by layer (LbL) technique. Nanosized Au nanoparticles were grown inside PAMAM molecules using formic acid as the reduction agent. The PAMAM – Au hybrids were then assembled onto an indium tin oxide (ITO) electrode.

The sequential deposition of LbL multilayers was carried out by immersing the substrates alternately into the PAMAM – Au and PVS solution for 5 min. After deposition of each layer, the substrate / film system was rinsed and dried with N_2 . The ITO covered with (PVS / PAMAM – Au)_n films where inserted into the electrochemical cell containing 0.5M H_2SO_4 at 293 K in presence of 5mM $\text{Fe}(\text{CN})_6^{3-}$ as electroactive species since 2h at open circuit developing cyclic and obtaining a cyclic voltammetry with 50 mVs^{-1} as scan rate, synthesizing the modified surface: ITO / PVS / PAMAM – Au @ PB (Figure 12) [99].

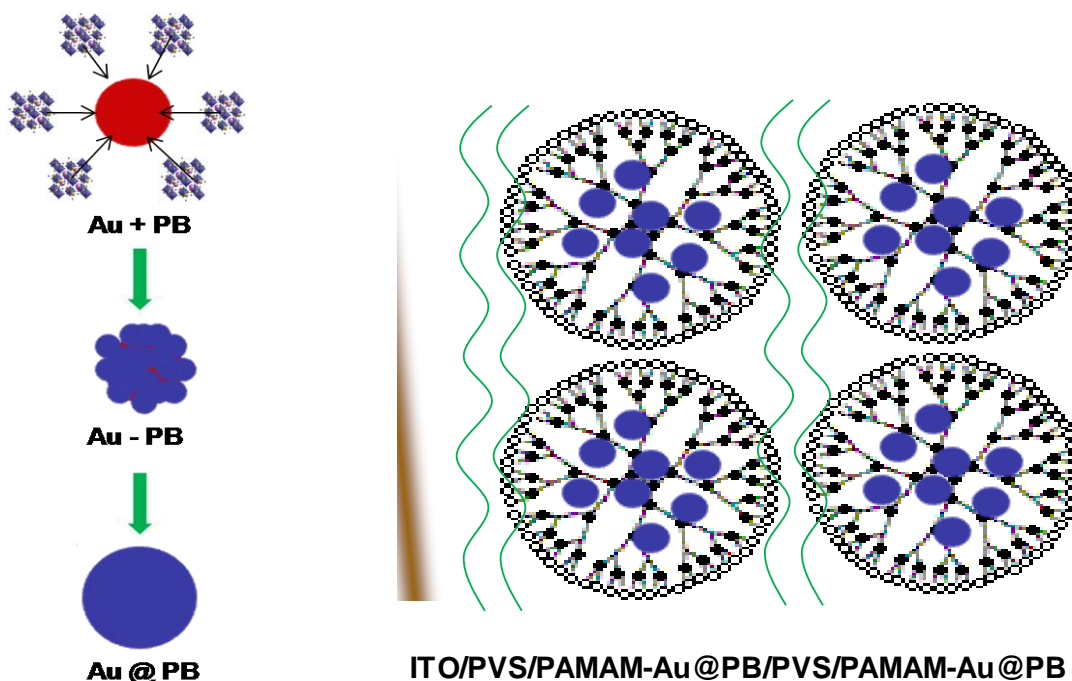


Figure 12. Schematic fabrication of LbL films comprising PVS and gold nanoparticles encapsulated in polyamidoamine generation 4 (G4 PAMAM) dendrimers.

4.2. Characterization of Modified Surfaces with Composites PB – PAMAM dendrimers.

For characterization purposes, the modified electrodes with PAMAM – PB these spherical gold bead electrodes were immersed in 0.5 mM $\text{Ru}(\text{NH}_3)_6\text{Cl}_3$ solutions in phosphate buffer pH 7 ($I=0.1$), and the geometric area was computed from the CV response of the reversible couple at different scan rates using the Randles-Sevcik equation [149]. The geometric area thus computed (around $0.02 \pm 0.005 \text{ cm}^2$) was considered to be the actual area, since electrodes prepared in this way have been reported to have roughness factors very close to unity [108].

The cyclic voltammetry has been used to determine the effective diffusion coefficient and the rate constant of ion transfer for a coupled transport of cations and electrons and their accessibility [22, 150]. Nevertheless, the PB films thickness, L , can be also estimated from the electric charge involved in the voltammetric experiments, as:

$$L = (Q/FA) (d^3N_A / 4)$$

Where Q is the electrical charge obtained from the voltammograms, A is the working electrode area, F is the Faraday constant ($96\,484.56 \text{ C mol}^{-1}$), d is the length of the unit cell (10.17 \AA) and N_A is the Avogadro’s number ($6.022 \times 10^{23} \text{ mol}^{-1}$). The value of 4 appears in the equation since there are four effective iron atoms in the unit cell [36].

As has been reported previously, the voltammetric response of PB films in aqueous potassium electrolytes (Figure 13), which consists of two sets of peaks corresponding to two reversible redox reactions of PB ($\text{Fe}_4^{\text{III}}[\text{Fe}^{\text{II}}(\text{CN})_6]_3$, between 0.2 to 0.9V vs. SCE): its reduction to Everitt's salt or Prussian White (PW, $\text{K}_4\text{Fe}_4^{\text{II}}[\text{Fe}^{\text{II}}(\text{CN})_6]_3$, $E < 0.2\text{V}$ vs. SCE) and its oxidation to Prussian Yellow or Green (PY, $\text{Fe}_4^{\text{III}}[\text{Fe}^{\text{III}}(\text{CN})_6\text{A}]_3$, $E > 0.9\text{V}$ vs. SCE), where A is the anion supplied by the electrolyte, the electrochemical reactions are [7, 13-16, 22, 151-152]:

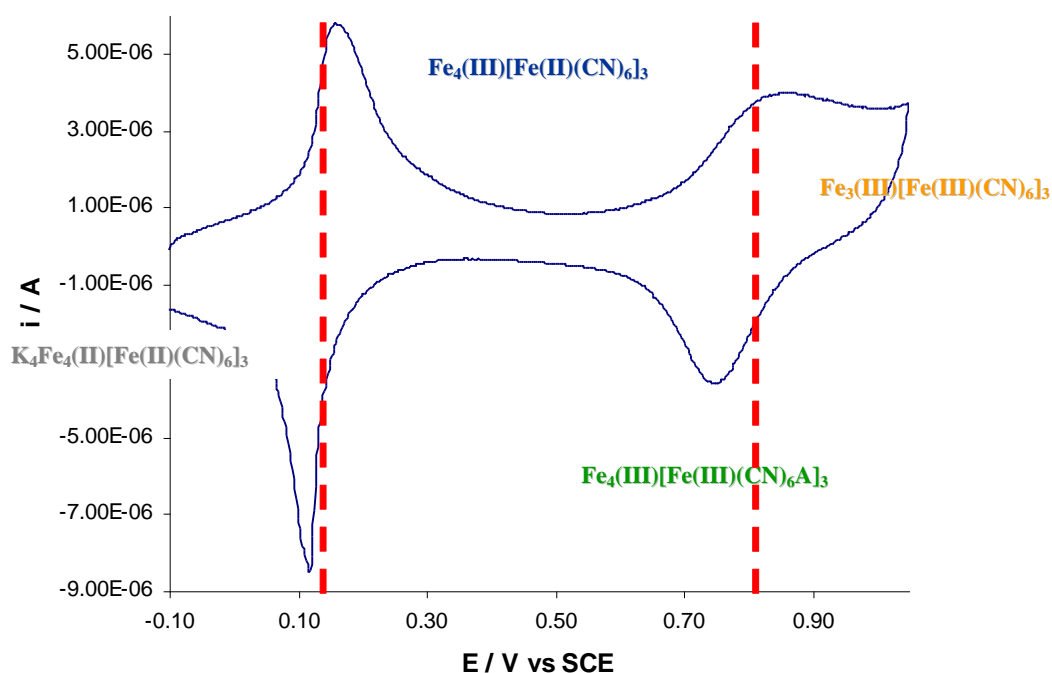
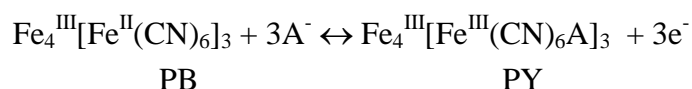
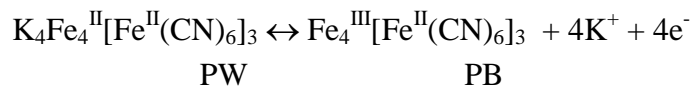


Figure 13. Cyclic voltammetry of PB in phosphate buffer pH 2 at 298 K.

The redox process at more negative potentials is caused by the iron coordinated to nitrogen (i.e., the high – spin iron), and the other corresponds to iron coordinated to carbon (i.e., low – spin iron) [13]. Both redox processes of PB involve the exchange of cations, usually monovalent alkali metal ions, between the solid compound and the solution: the expulsion of these cations from the PB lattice to the solution during oxidation and their uptake during reduction [153].

Quantification of PB loading on the modified surfaces was carried out by computation of surface coverage values (Γ , mol cm^{-2}) obtained by integrating the current observed in the cathodic peak of each of the cyclic voltammograms shown in Figure 9, where $\Gamma = \Gamma (idt / fnFA) = Q / fnFA$, Q is the charge in coulombs, f is the roughness factor (1.1), n is the number of electrons involved in the

process, F is the Faraday constant ($96\,485\text{ C mol}^{-1}$), and A is the geometric area of the working electrode in cm^2 .

Comparing the answer of Au-SH-PGx-PB at different pH values, no PB electrochemically related signals could be identified in any of the substrates prepared at pH 12, since under these conditions PB readily dissociates into $\text{Fe}(\text{OH})_3$ and $\text{Fe}(\text{CN})_6^{4-}$ (Figure 14) [154-155].

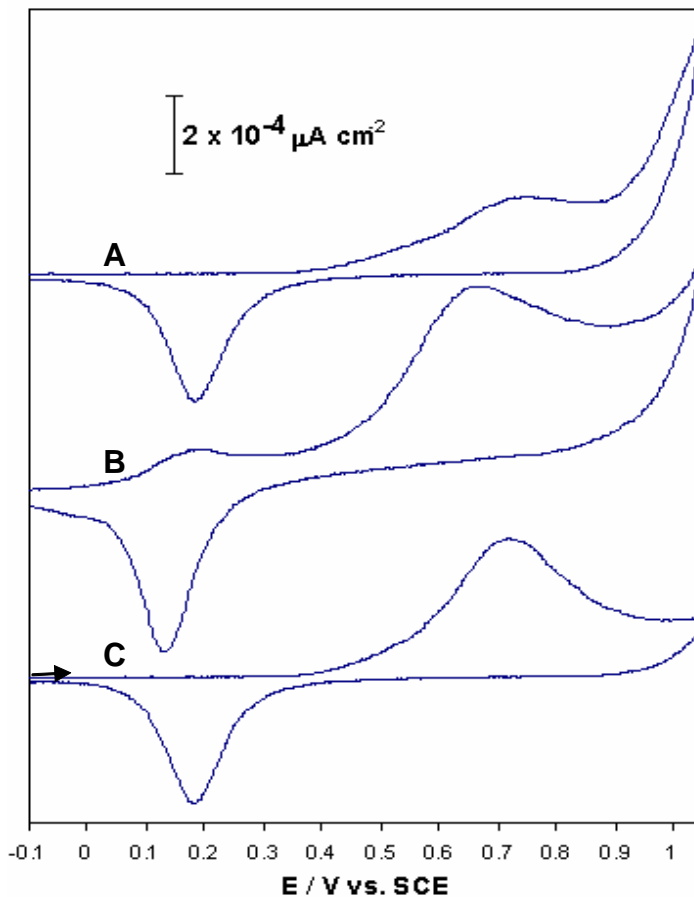


Figure 14. Cyclic voltammograms of Au (A), Au - PG3.5 - PB (B) and Au - SH - PG4 - PB (C) in phosphate buffer pH 12 ($i = 0.1$), at 0.1 V s^{-1} and 298 K.

In other hand, the formation of PB species at pH values smaller than 5 was expected, as it has been thoroughly reported in the literature [2, 21, 134], but PB films are known to be unstable at neutral pH conditions.

But, at pH 7 values, only the modified electrodes with dendrimers (Au - SH - PG4.0 - PB) showed the electrochemical signals of PB, where PG4.0 had a higher coverage of PB than PG3.5 (Figure 10 - B), in consequence of pKa values in solution are 9.52 [156] and 3.79 [157] respectively.

So, the PAMAM G4.0 at $\text{pH} < 9.52$ has a local acidic conditions at the electrode - solution interface (Figure 15).

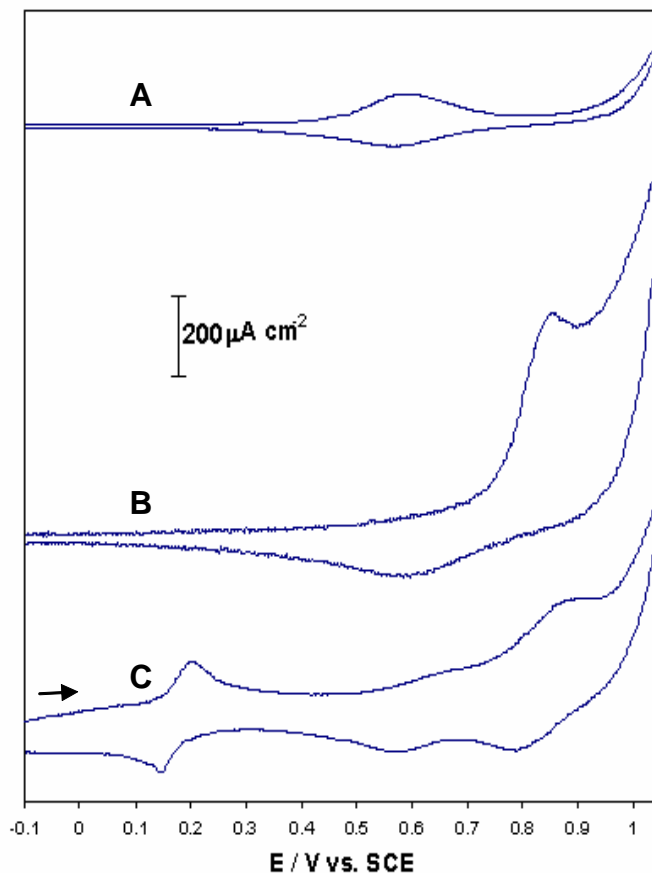


Figure 15. Cyclic voltammograms of Au (A), Au - PG3.5 - PB (B) and Au - SH - PG4 - PB (C) in phosphate buffer pH 7 ($i = 0.1$), at 0.1 V s^{-1} and 298 K.

This behavior demonstrate that PB molecules are actually confined to the electrode surface as a consequence of the dendrimer protonated state that, by virtue of the pK_a of the peripheral functional amine groups ($-\text{NH}_3^+ / -\text{NH}_2$, $pK_a = 9.52$) [156], must result in a localized low pH value at the electrode - electrolyte interface even under neutral bulk solution conditions. This asseveration can be validated at pH 2, PB was preferentially adsorbed on the two dendrimer containing electrodes, since the coverage (Γ) values calculated are roughly equal to each other and about 7 times larger than those obtained in unmodified gold electrodes on which PB was confined (Figure 16), where the highest density of current of PB was using Au - SH - PG4.0 - PB (Figure 16-C).

EIS has proved to be the best suitable technique to separate the processes with different relaxation time constants which take place in the electrochemistry of these films [158]. It is very common to analyze the impedance results by means of equivalent circuits [159], where the values of the electrical components are associated with the physical / chemistry properties of the electrochemical systems [160].

In the past few years, impedance spectroscopy or EIS have been revealed as useful tools in the study of charge transport processes in conducting films, and in particular, in electrodeposited films of PB. These techniques have been used to obtain more detailed information about the transport of

charged species during the redox reactions of these systems [22], or the diffusion of K^+ ions between the vacuum spaces of the PB [22, 161-163].

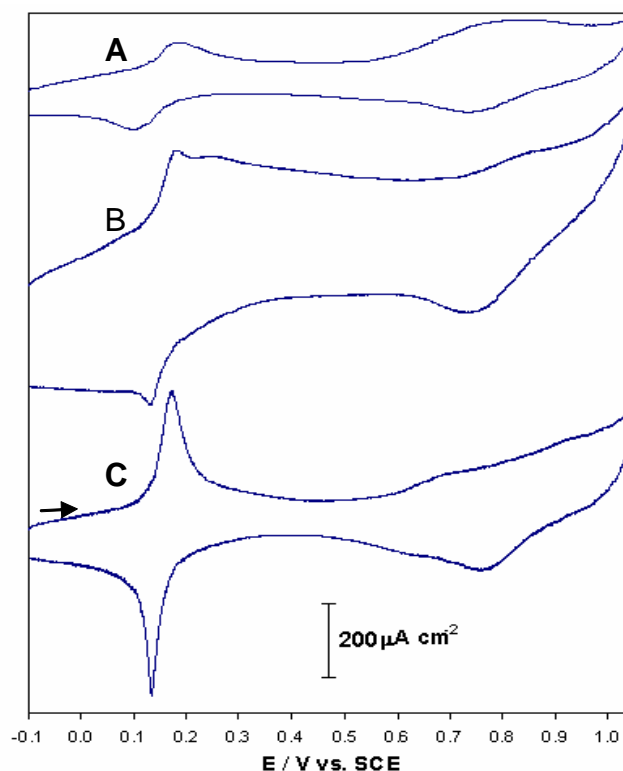


Figure 16. Cyclic voltammograms of Au (A), Au - PG3.5 - PB (B) and Au - SH - PG4 - PB (C) in phosphate buffer pH 2 ($i = 0.1$), at 0.1 V s^{-1} and 298 K.

In the case of a film - modified electrode where the electroactive species is assumed to be fixed at the surface of the electrode, the impedance spectra could be represented by the Randles's modified equivalent circuit, which contains two transmission lines associated in parallel. These lines are a finite length transmission line and semi-infinite Warburg impedance, respectively, to correspond to a fast and a slow charge transport processes across the lamellar materials. The ideal double-layer capacity is replaced by a constant phase element (CPE), which reflects the double-layer capacitance at the first PB layer interface [22].

Comparing the covalent (Figure 17 - C) with the electrostatically (Figure 17 - B) modified electrodes, the stability and major presence of the PB was observed with the increase of the capacitance at high frequencies, as the Au - SH - G4.0 - PB showed, in contrast the naked gold electrode (Au, Figure 17 - A). Although, the diffusion of the ions presents in solution across the interface was similar in all the different surfaces.

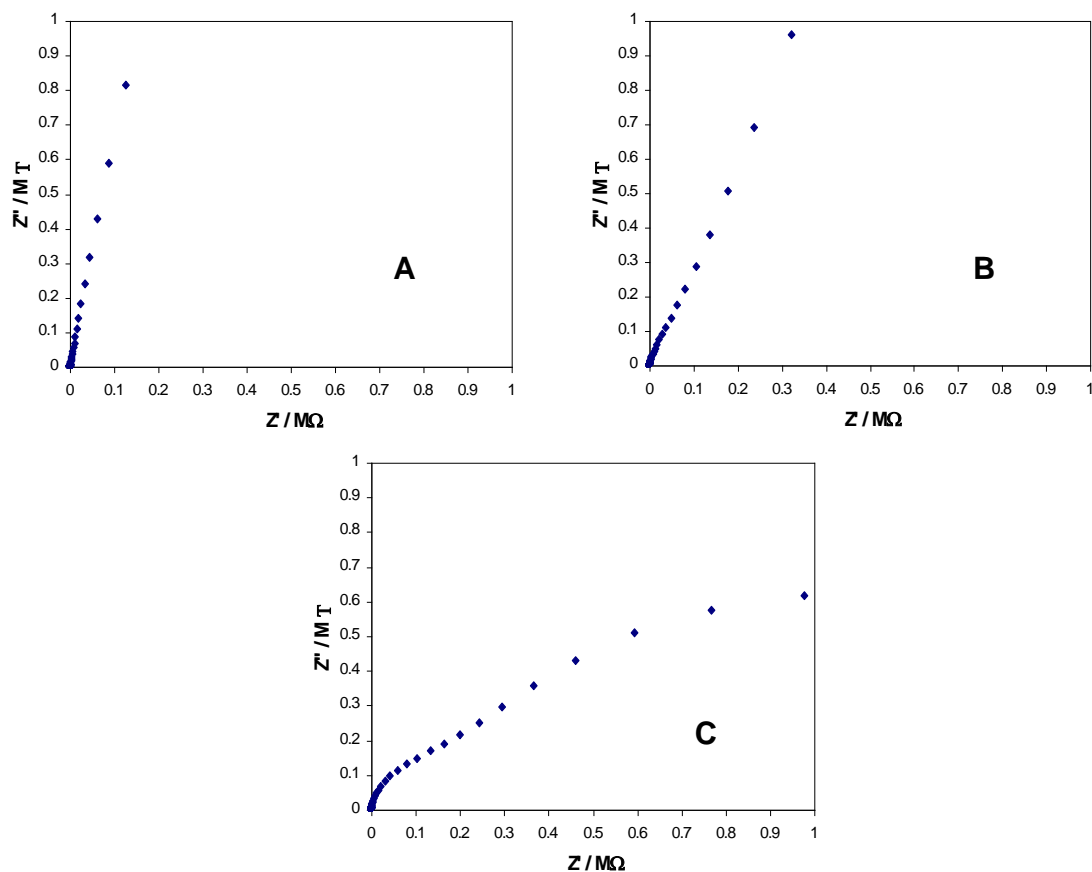


Figure 17. Nyquist spectra of Au (A), Au – PG4.0 – PB (B) and Au – SH – PG4.0 – PB (C) in phosphate buffer pH 2 ($i = 0.1$) with 1mM of ferrocyanide, using the equilibrium potential at 298 K with nitrogen atmosphere, between 0.1 Hz to 100 kHz with 10mV of amplitude and 500 points of acquisition.

The EQCM has been widely used to study the ion and solvent transport behavior during the redox reaction of a film [11, 16, 164-166]. The comparison between mass change (ΔM) and current (I) gives important information on the identity of charge compensating species. Moreover, when isotopically labeled solvent is used, the contribution of ion and solvent to the total mass transport can be separated [167]. Finally, the EQCM measures the current response to the small potential perturbation [168-170].

Using this technique, from the comparison between charge change and mass change responses during the electrodeposition of the PB film, it was found quantitatively that the PB film is highly hydrated and that it undergoes an irreversible mass change during the first cathodic scan, which evidently results from the structural reorganization of the PB film from the insoluble form to the soluble form. In addition, substantial amount of water molecules escapes the PB film during the structural reorganization. In the steady-state mass transport of the PB film, the identity of the transporting species is nearly invariant over the entire potential range and the electrolyte cation plays a major role in the ion transport [16, 171].

By measuring the redox charge consumption of the PB thin film or the mass gain after the deposition with an EQCM, both deposition efficiencies can be calculated. The porosity and the apparent density can be calculated, and the come in and out of different cations [16].

The EQCM can be used to calculate the deposition efficiency in two different ways: (1) deposition efficiency based on the charge consumption, η_q , and (2) deposition efficiency based on the mass gain, η_m , which can be defined as follows:

$$\eta_q = (\text{charge consumed during the reduction of PB to ES}) / (\text{charge consumed during the deposition}) \times 100\%.$$

$$\eta_m = (\text{actual mass gain measured during the deposition}) / (\text{theoretical mass gain during the deposition}) \times 100\%.$$

η_q is a measure of the percentage of total charge passed to the electrode to form the Fe^{3+} sites in the PB lattices during PB deposition as judged by the PB reduction to form ES. η_m is a measure of the difference between the expected and the actual mass gain during PB deposition. For the estimation of η_q , the charge consumed during the reduction of PB to ES can be estimated by performing cyclic voltammetry (CV) or potential – step (PS) experiments [16].

The porosity of the PB thin film, ξ , can be estimated with this technique as follows:

$$\xi = 1 - [(\text{theoretical film thickness calculated}) / (\text{actual film thickness measured})]$$

The practical meaning of porosity for a thin film implies the percentage of the thin film volume which is porous, or filled with open spaces. Assuming that there is no defect in the PB lattice structure and that a 100% Faradaic efficiency occurs for the reduction of PB to ES without involving any side reactions, the theoretical film thickness of the PB can be calculated to be 1140 Å [16].

Further evidence of the PB level on the electrode surfaces can be obtained from examination of modified gold CD-trodes by FT-IR spectroscopy (Figure 18) [108], which are modified by immersion of the surface in PB solution at acid pH since 24 h.

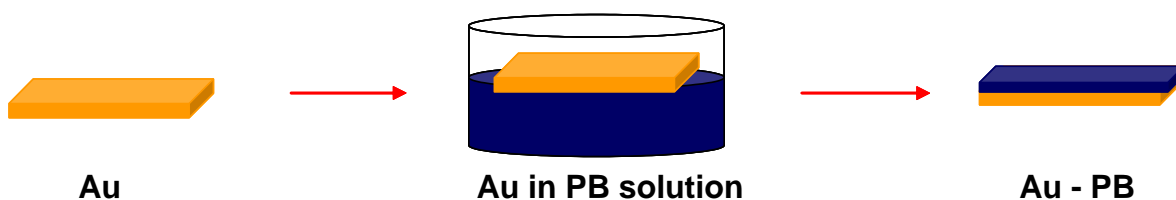


Figure 18. Schematic representation of modified gold CD-trodes with PB solution.

Over other kind of materials, as hexacyanoferrate – doped silica sol- gels processed to contain PAMAM G4.0, have been study with this technique [142]. The FT-IR spectra show characteristic PB peaks at 2090 cm^{-1} associated with the vibrational frequencies of the bridging cyanide ligands in PB [14, 135, 172-173], the intensity of which increase proportionally with the generation of dendrimer present (Figure 19). Furthermore, the PB signal those for the comparable dendrimer physically adsorbed (Figure 19 – A). The covalent modified electrodes showed more higher intensities (Figure 19

- B) than electrostatically modification for the different dendrimer generation. In this manner, Au – SH – PG4 – PB provided the strongest signal by the highest coverage of PB of surfaces compared.

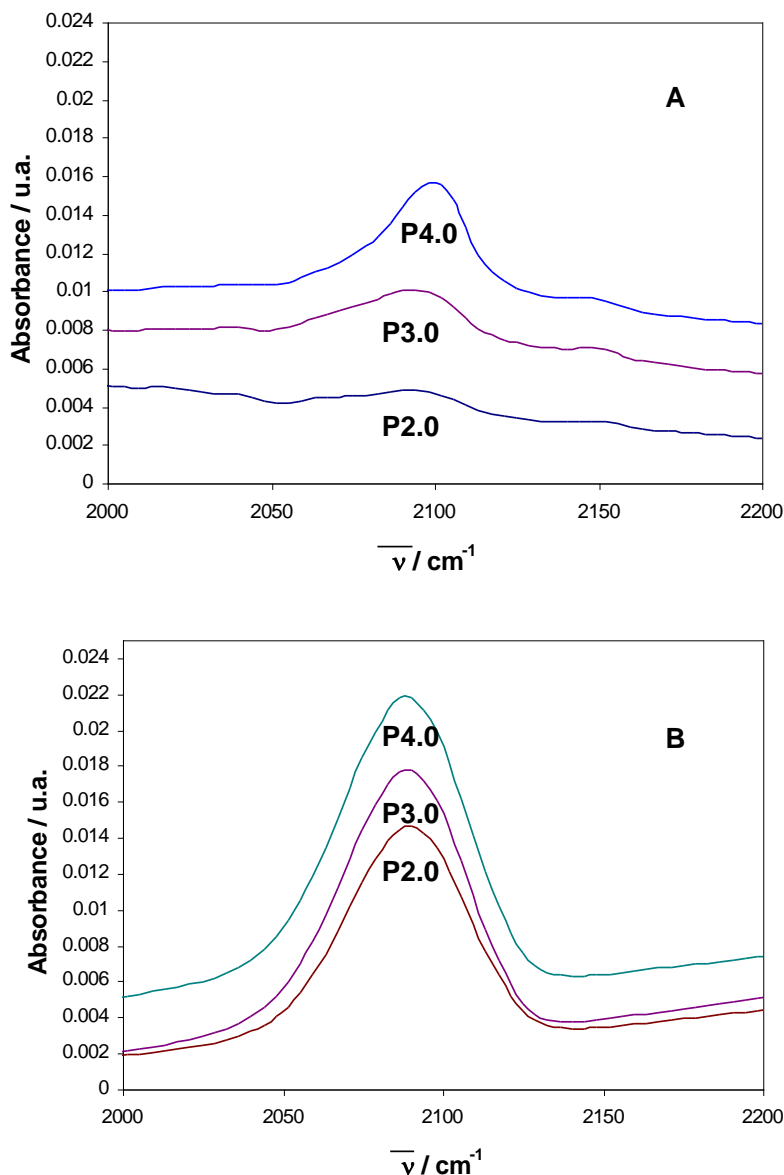


Figure 19. FT-IR spectra with specular reflectance technique at 45° the light with p-polarized light with 250 individual scans of different electrostatic (A) and covalent (B) modified electrodes with PAMAM generation 2.0, 3.0 and 4.0 at 298 K.

With Raman Spectroscopy, the modified surfaces of PAMAM – PB can be analyzed, across the characteristic signal of PB around 2089, 2125 and 2147 cm^{-1} [174-175], which have been assigned to the Raman vibrational frequencies of the bridging cyanide ligands in PB, across of the structure $\text{Fe}^{3+} - \text{C} \equiv \text{N} - \text{Fe}^{3+}$ [174-177], In this manner, the homogeneity of PB film was showed with PAMAM G4.0, in consequence its Raman signal was the highest than PAMAM G3.5 – PB and PB (Figure 20-1).

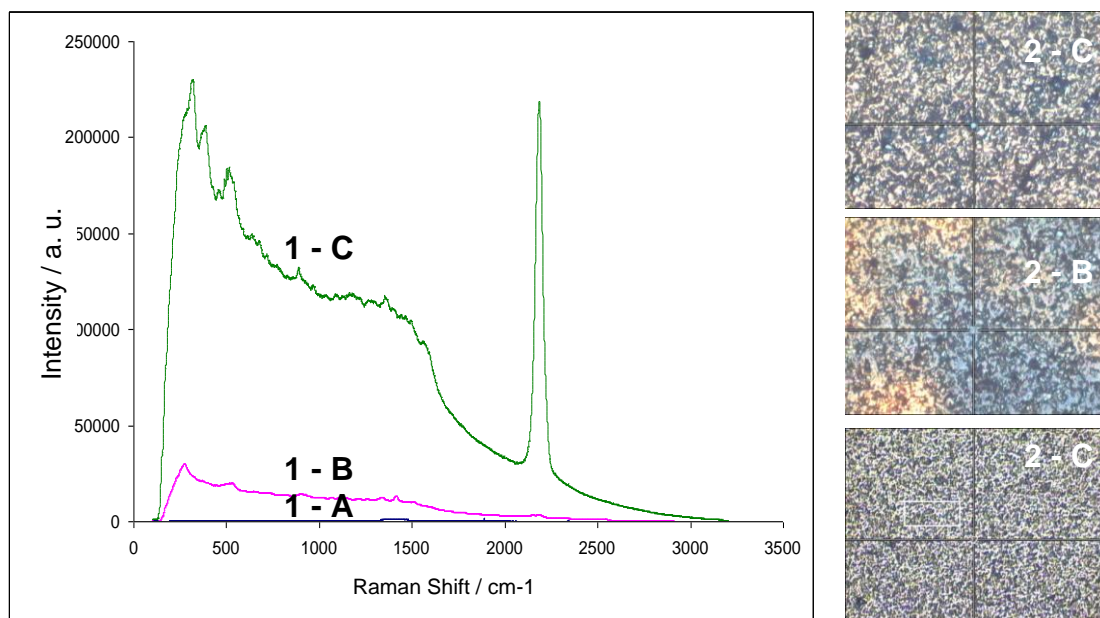


Figure 20. Raman spectroscopy (1) and optical image (2) at 50x of PB (A), PB – PAMAM G3.5 (B) and PAMAM G4.0 (C).

Making a mapping of different surfaces: Au - PB, Au – SH – PG3.5 – PB and Au – SH – PG4.0 – PB, for each 2 μm point along a 18 μm line randomly selected on each electrode, substrate, the integration of the peaks in the 1950 to 2200 cm^{-1} range was performed (Φ). The resulting integration values were divided by the largest integration value obtained in each substrate (Figure 21) Whereas the square markers and the boxes shown in figure represent the mean fractional integrated values and the zone in which 7% of the data falls, respectively, the extreme points of the vertical lines indicate the maximum and minimum fractional values that were obtained for each substrate. The difference between the largest and smallest fractional integrated values (i.e., the maximum dispersion of the data samples) is larger for the Au – SH – PG3.5 – PB than Au – SH – PG4.0 – PB modified electrode and also smaller than that measured for the Au – PB surface [107].

To study the morphology and distribution of PB on modified surfaces, EDX and SEM technique are used. For developed these techniques, the surface measurements were made over a planar gold-film electrodes from recordable CDs (gold CD-trode, Kodak, México) can be used as substrate [178-179], modifying with PB in the same manner as the spherical gold bead electrodes.

In this manner, comparing different modified electrodes with different generations of dendrimers and PB, the most uniform distribution and the highest coverage of nanostructure PB were achieved with covalently bond PAMAM G4.0 (Figure 22).

X-ray absorption spectroscopy (XAS) is used as a local structural tool. The technique is sensitive to short-range order (a few angstroms, around the selected atom) and can be applied to disordered, amorphous and crystalline materials [132].

This technique is developed usually over glass surface with low concentration of Prussian compounds. The use of XAS appears to be very useful to determine the local structure of Prussian

reactive that react with the surface. These measurements are carried out in the fluorescence detection mode at metal sites, thereby allowing a double internal structural and electronic probe [6].

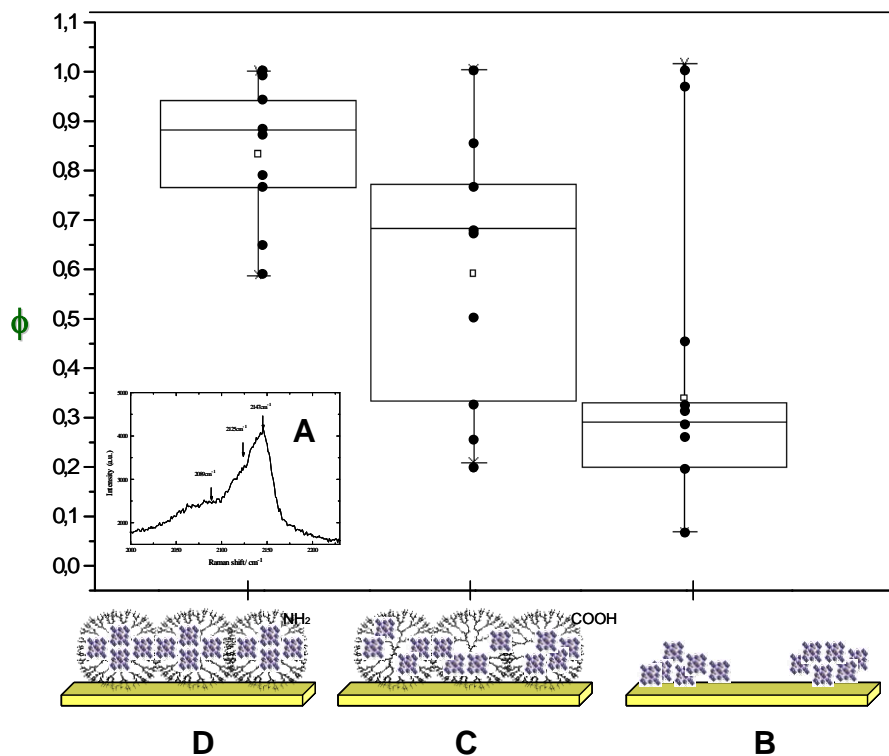


Figure 21. Schematic distribution of PB integral fraction peak intensities, ϕ , of a linear Raman spectroscopy mapping (A) for: PB (B), Au – SH – PG3.5 – PB (C) and Au – SH – PG4.0 – PB (D).

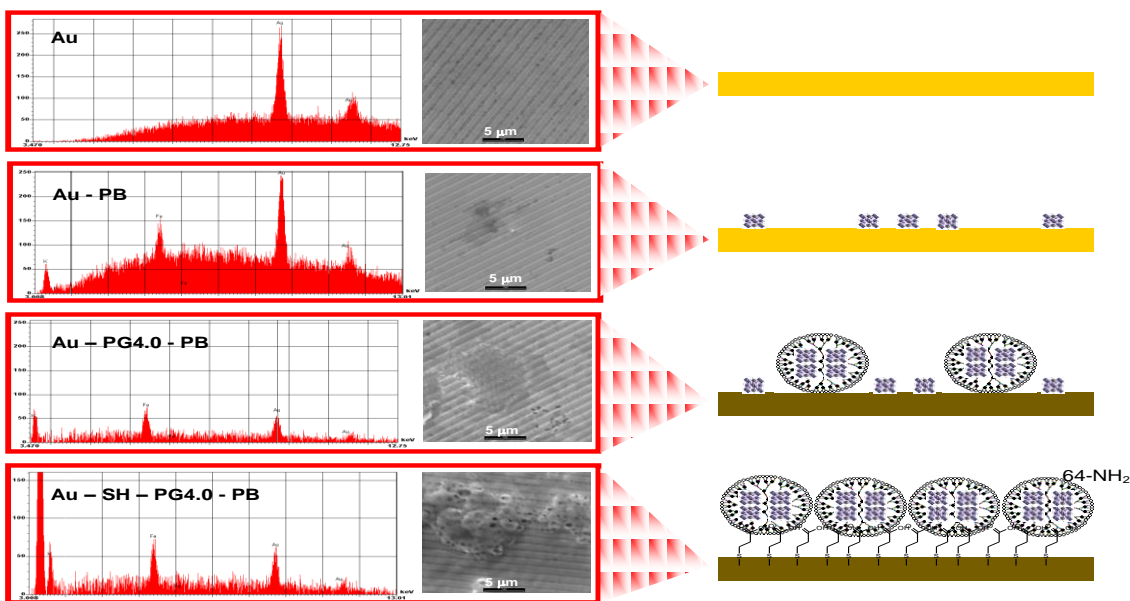


Figure 22. Microanalysis with EDX and image of SEM results for Au, Au – PB, Au – PG4.0 – PB and Au – SH – PAMAM G4.0 – PB modified CD – trodes. Experiments obtained with an accelerating voltage of 15kV and with a magnification of 2 000 x.

5. APPLICATION OF THE MODIFIED SURFACES WITH NANO-STRUCTURED COMPOSITES OF PRUSSIAN BLUE AND DENDRIMERS.

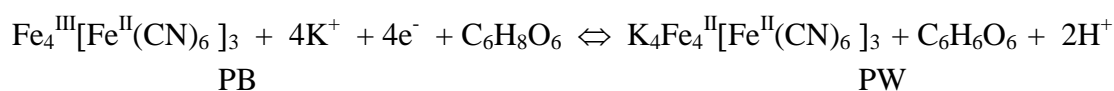
Prussian Blue in the form of a film on solid electrodes, many studies of the electrochemical behavior of such films have been performed. It has been shown that electrodes modified with PB and related cyanometalate compounds exhibit many interesting properties that make them potentially applicable in areas such as ion-selecting sensors [180-182], electrocatalysis [28, 88, 183-187], membranes [1, 188], electrochromism [30, 44, 189-191], solid state batteries [6, 38, 188-193], molecular magnetism [194], photosensing devices, and energy storage [22].

Peroxide hydrogen (H₂O₂) and dopamine (DA), play important roles in the functioning of the central nervous system [195]. They offer the most valuable clinical markers for oxidative stress, recognized as a major risk factor in the progression of disease-related pathophysiological complications in clinical diagnostics [2, 20, 70, 134, 196-197]. This is the motivation for monitoring both compounds at very low levels of concentration.

5.1. Electro-oxidation of Ascorbic Acid.

Ascorbic Acid (AA) or Vitamin "C" is present in vegetables, citric fruits and animals tissue. It is essential for the development and regeneration of muscles, bones, teeth and skin. It has also been used for the treatment of the common cold, mental illness, infertility, cancer and AIDS [196, 198]. This compound has biological interest because it is used as co-enzyme or cofactor, with a high antioxidant action [70, 199].

PAMAM dendrimers and PB on surface, have been used to electro-oxidized AA in aqueous medium [20], with the next general reaction, where the Fe(III) ions in PB, are the responsible of the electro-catalytic effect for the transference of 4 mol of e⁻ [2, 20, 70, 134, 196, 200-202]:



PB films have a catalytic effect on the anodic electrochemical response of ascorbic acid (AA) that is reflected by a substantial increase in the related oxidation current density around 0.6 V vs. SCE (Figure 23) [203].

Electrochemical detection of AA can be developed at pH 2 and 7 under constant stirring conditions (900 rpm) at a constant applied potential of 0.8 V vs. SCE (a potential sufficiently anodic to oxidize the AA molecules on any of the substrates surveyed) and at different concentrations of AA in the 0 – 120 μM, the concentration range showed linear response ($r^2 > 0.99$) for the limiting current densities, J, versus AA concentration with different slopes for all the substrates considered (Table 2).

At pH 2, the Au – SH – Px – PB were the most sensible to detect AA with about 3.5 times larger the slope as compared to that observed for clean gold substrates and approximately 2 times more higher than those obtained using any of the Au – SH - PB modified electrodes. PB – dendrimers showed practically the same detection and quantification limit each other. This phenomenon is

because the PB - dendrimer interaction is essentially independent of the dendrimer peripheral functionalities and, therefore, must be taking place within the hyper - ramified polymer [204-205].

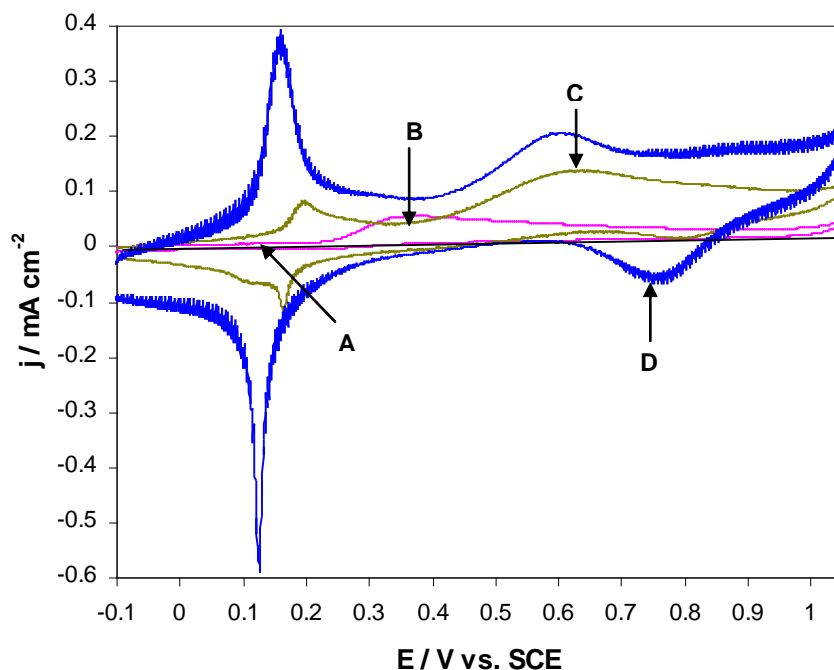


Figure 23. Cyclic voltammeteries of the electro-oxidation of 0.1M AA in phosphate buffer pH 2 ($I=0.1$) over: Au (A), Au + AA (B), Au - PB + AA (C) and Au - SH - PG4.0 - PB (D) at 0.100 V s^{-1} and 298 K.

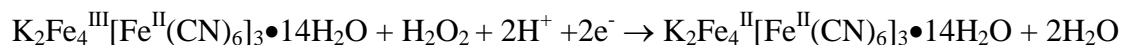
At pH 7, the Au - SH - PG4.0 - PB substrate showed a substantially larger slope (about 20 times) than those observed for all the other surfaces under study, a fact that not only reflects the presence of the electrocatalytic PB film on the electrode surface but also results in an improved D.L. and Q.L. (Table 2 and Figure 24) when compared to the other modified electrodes. It is the unique heterogeneous film capable of stabilizing PB on the electrode surface and maintaining at the same time the necessary permeability to keep the interface accessible to electroactive species in solution [206].

5.2. Electro-reduction of Hydrogen Peroxide.

The hydrogen peroxide (H_2O_2) is very used in medicine, environmental control and industrial activities (textile, paper, food, mill and oil) [202, 207-209]. At the other hand, H_2O_2 is the most valuable marker for oxidative stress, recognized as one of the major risk factors in progression of disease-related pathophysiological complications in diabetes, atherosclerosis, renal disease, cancer, aging, and other conditions.

PB has been defined as an “artificial peroxidase” because of its analogy with the biological family of peroxidase enzymes, responsible in nature for reduction hydrogen peroxide [71-72, 210-213]. The reduction H_2O_2 reaction in presence of PB is present [151], where the reduction of hydrogen

peroxide is really catalysed by the ferric ions, in the film followed by electron transfer to H_2O_2 molecules from Fe^{2+} , centers in the PB film [214]. The electrochemical reaction of H_2O_2 with PB with the transferred of two electrons in neutral conditions, is defined as [2, 21, 28, 148, 199]:



Taking into account that H_2O_2 reduction in neutral solutions by selective Prussian blue is a two – electron process yielding hydroxide ions one can postulate an overall reaction for the electrocatalytic process [2, 72, 148]:

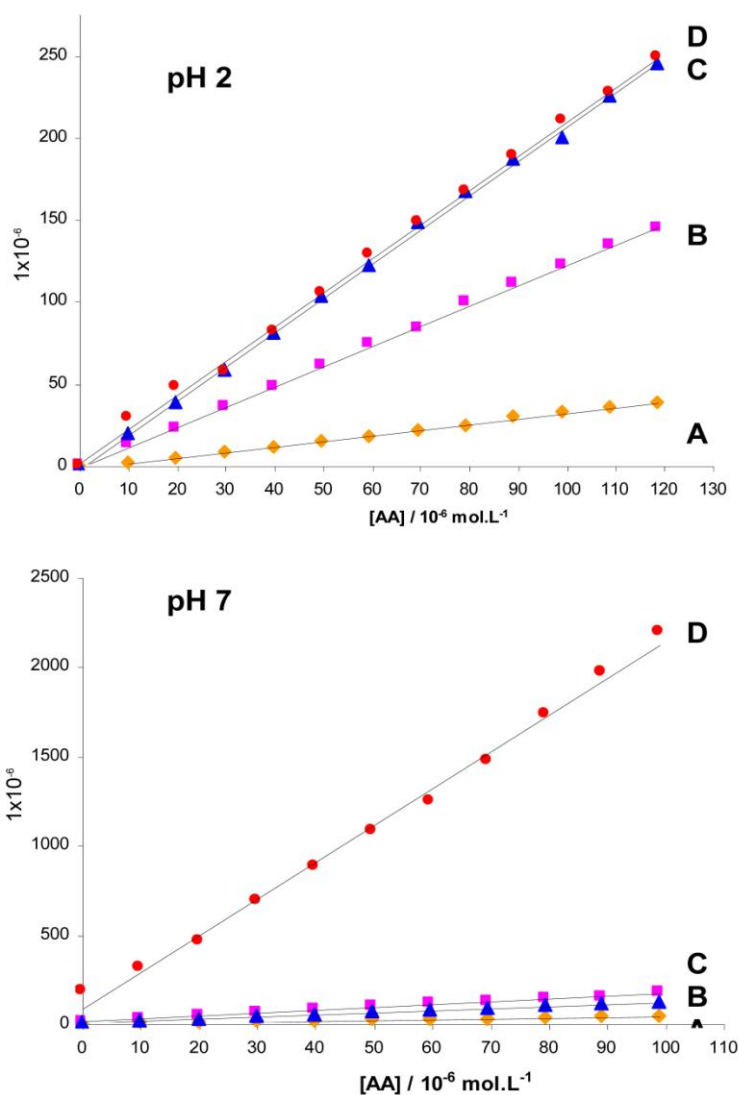


Figure 24. Curves of J vs. $[\text{AA}]$ in the 0 – 120 μM concentration range obtained in phosphate buffered pH 2 and 7 aqueous solution ($I=0.1$), under constant stirring (900 rpm) and an applied potential of 0.8V vs. SCE using Au (A), Au – PB (B), Au – SH – PG3.5 – PB (C) and Au – SH – PG4.0 – PB (D).

Table 2. Surface coverage (Γ), detection (D.L.) and quantification limits (Q.L.) of ascorbic acid obtained with gold electrodes modified with dendrimers and PB. D. L. = Detection Limit = $3 \sigma / m$ and Q. L. = Quantification Limit = $10 \sigma / m$, where σ is the standard deviation of noise and m as the slope to the lineal relationship.

Detector	Γ , $10^{-10} \text{ mol cm}^{-2}$	Linear Equation, $y[\mu\text{A}] = mx[\mu\text{M}] + b$	r^2	D.L. μM	Q.L. μM
pH 2 (I = 0.1)					
Au	0	$0.34 [\text{AA}] - 1.64$	0.9966	33.19	110.62
Au – PB	1.02	$1.24 [\text{AA}] - 0.69$	0.9993	9.10	30.34
Au – SH – PG3.5 – PB	7.28	$2.08 [\text{AA}] + 2.28$	0.9982	5.41	18.03
Au – SH – PG4.0 – PB	7.58	$2.08 [\text{AA}] - 1.41$	0.9989	5.40	18.01
pH 7 (I=0.1)					
Au	0	$0.43 [\text{AA}] + 1.80$	0.9944	111.95	373.15
Au – PB	0.63	$1.58 [\text{AA}] + 13.52$	0.9987	30.13	100.42
Au – SH – PG3.5 – PB	2.73	$1.17 [\text{AA}] + 7.80$	0.9976	40.64	135.47
Au – SH – PG4.0 – PB	2.85	$20.60 [\text{AA}] + 87.18$	0.9944	2.32	7.72

The electrocatalytic reduction of H_2O_2 at Au / PB, Au / MPA / PAMAM / PB and Au / MPA / PAMAM / nano – Au / PB was studied by chronoamperometry at -0.2V , where the last surface modified had the highest sensitivity by the highest diffusion coefficient showed during the electro-reduction of H_2O_2 ($1.94 \times 10^{-5} \text{ cm}^2 \text{ s}^{-1}$) at near neutral aqueous solution (figure 25) [107, 148].

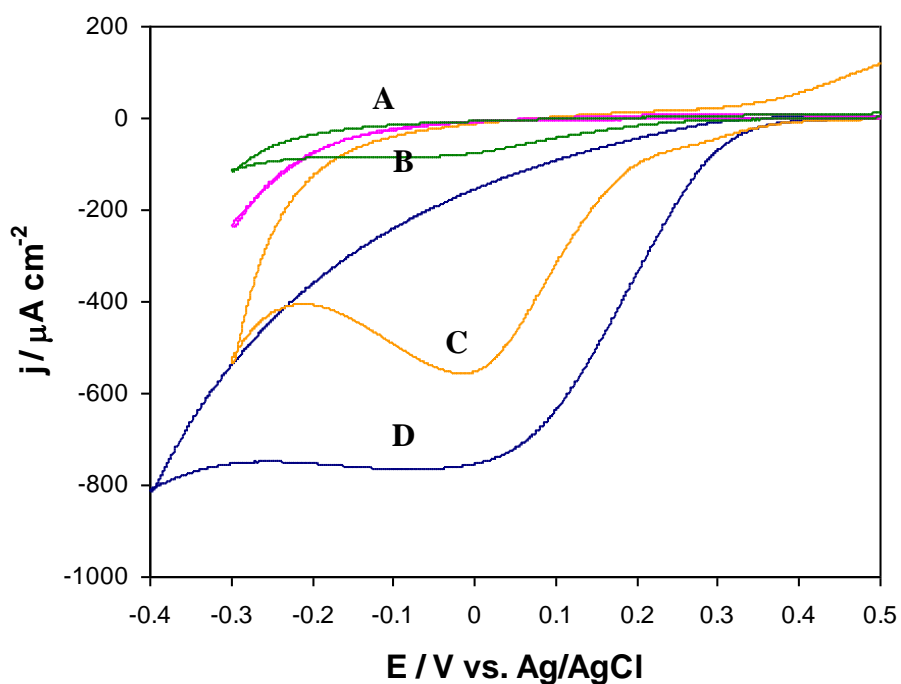


Figure 25. Cyclic voltammogram for the electro-reduction of $15 \mu\text{M}$ H_2O_2 over electrodes: Au (A), Au – PB (B), Au – PG4.0 – PB (C) and Au – SH – PG4.0 – PB (D) at 0.02 V s^{-1} and 298 K .

To test the electrocatalytic properties of the modified electrodes, we obtained the CV response of 15 μM H_2O_2 in 0.1 M KCl to observe the H_2O_2 reduction reaction [28, 175]. In these experiments (Figure 25), the covalently modified electrode coated with PAMAM G4.0 and PB presented the highest electrocatalytic currents in KCl medium (Figure 25-d), as consequence of the highest PB coverage as demonstrated in the previous experiments. The electrochemical reduction of hydrogen peroxide clearly depends on the amount of the Prussian Blue deposited on the electrode surface.

In this manner, the cathodic current increases with the higher generation of dendrimer, with both physically and chemically bound dendrimer at different electrolytes, as phosphate buffer pH 7 and 0.1M KCl. For the same generation of dendrimer, the currents were greater for the covalently modified electrodes, indicating greater coverage by PB. With no dendrimer present, no PB current is obtained on Au electrodes and a very small response is detected with the Au – SH modified surface. Furthermore, it is seen that the currents obtained with the KCl solution (figure 26 – b) are generally much larger than those with the phosphate buffer (Figure 26 – a and table 3).

Table 3. Surface coverage (Γ), detection (D.L.) and quantification limits (Q.L.) of hydrogen peroxide obtained with gold electrodes modified with dendrimers and PB, using 0.1M KCl. D. L. = Detection Limit = $3 \sigma / m$ and Q. L. = Quantification Limit = $10 \sigma / m$, where σ is the standard deviation of noise and m as the slope to the lineal relationship.

Detector	Γ , $10^{-10} \text{ mol cm}^{-2}$	Linear Equation, $y[\mu\text{A}] = mx[\mu\text{M}] + b$	r^2	D.L. μM	Q.L. μM
Au	0	1.9137 $[\text{H}_2\text{O}_2]$ – 0.6844	0.9865	5.0008	16.6693
Au – PB	0	2.0876 $[\text{H}_2\text{O}_2]$ – 0.9818	0.9886	4.5852	15.2807
Au – PG2.0 – PB	8.86	2.6741 $[\text{H}_2\text{O}_2]$ – 1.2640	0.9882	3.5788	11.9292
Au – PG3.0 – PB	12.15	3.7350 $[\text{H}_2\text{O}_2]$ + 3.6135	0.9827	2.5622	8.5408
Au – PG4.0 – PB	13.25	5.5057 $[\text{H}_2\text{O}_2]$ + 1.8937	0.9960	1.7382	5.7940
Au – SH – PG2.0 – PB	19.04	7.6060 $[\text{H}_2\text{O}_2]$ + 4.6092	0.9895	1.2582	4.1941
Au – SH – PG3.0 – PB	23.30	10.8370 $[\text{H}_2\text{O}_2]$ + 5.7106	0.9953	0.8831	2.9436
Au – SH – PG4.0 – PB	28.31	30.2890 $[\text{H}_2\text{O}_2]$ – 6.7094	0.990	0.3160	1.0532

The covalent electrode Au – SH – PG4 – PB in 0.1M KCl showed the greatest coverage of PB, with an increase of two times over the coverage of its reference, Au – PG4 – PB, and seven times larger than in the buffer solution [215-216]. This result is presumably a consequence of the higher ionic mobility of hydrated K^+ across the PB when KCl was used than hydrated Na^+ in the case of the buffer solution.

Once the electrocatalytic effect was confirmed, amperometric experiments were carried out at a constant applied potential of -0.1 V vs. Ag/AgCl (a potential sufficiently cathodic to reduce the H_2O_2 molecules on all of the substrates surveyed), and under constant stirring conditions. From these experiments we constructed calibration curves, which showed linear responses ($r^2 \cong 0.9$) for the current density j vs H_2O_2 concentration. The results are shown in Figure 26, and the detection (D.L.) and quantification limits (Q.L.) obtained are given in Table 3 [217].

The j vs H_2O_2 concentration response of the covalently modified gold electrodes coated with G4.0 PAMAM – PB shows a slope (related directly to sensitivity, figure 29 – b - 9) about 15 times larger than that obtained with bare gold substrates in 0.1 M KCl. The sensitivity of the amperometric response increases proportionally with molecular size and the number of functional groups of the dendrimer used. These results suggest that PB tethered by the support of amine dendrimers on gold substrates can be used at neutral pH to detect electroactive species in solution, such as H_2O_2 .

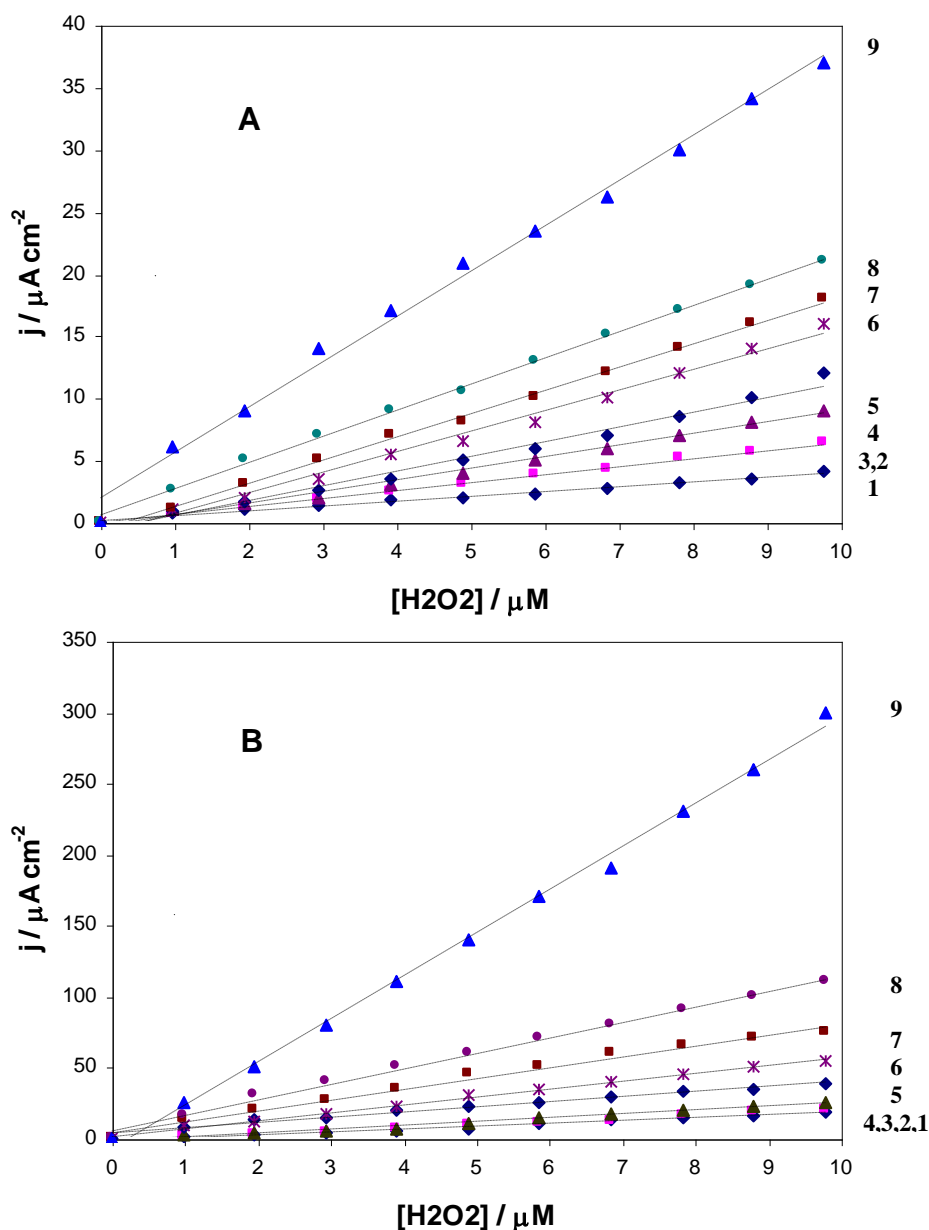


Figure 26. Cyclic voltammograms for the electro-reduction of 15 μM H_2O_2 over electrostatic and covalently modified gold electrodes: (1) Au, (2) Au – PB, (3) Au – SH – PB, (4) Au - PG2 – PB, (5) Au – PG3 – PB, (6) Au – PG4 – PB, (7) Au – SH – PG2 – PB, (8) Au – SH – PG3 – PB, (9) Au – SH – PG4 – PB, in phosphate buffered solution pH 7 (A) and 0.1 M KCl (B) at 0.02 V s^{-1} and 298 K.

6. CONCLUSIONS

The composites of PB – PAMAM dendrimer can be synthesized over the gold surface, which represent a new kind of modified electrodes in covalent or electrostatically manner to be used as electrocatalizer to detect molecules with biological importance.

The electrocatalysis is proportional with the increase of dendrimer generation, where the covalent modified electrodes are more sensible and selective than electrostatically modified electrodes.

In this sense, the best electrocatalyst was the electrode modified with dendrimer PAMAM G4.0, with terminal amines, getting the high sensitivity and selective, with low detection and quantification limits (on the order of μM) to detect molecules with biological importance as ascorbic acid and hydrogen peroxide.

ACKNOWLEDGEMENTS

The authors are grateful to Consejo Nacional de Ciencia y Tecnología (CONACYT) by the financial support across Grant 45157, J-34095 - E, Fondo Sectorial de investigación para la Educación - Ciencia Básica – 84955 and Fondo Mixto del Gobierno del Estado de Veracruz de Ignacio de la Llave – 96313.

References

1. M. Pyrasch, A. Toutianoush, W. Jin, J. Schnepf and B. Tieke, *Chem. Mater.*, 15 (2003) 245-255.
2. A.A. Karyakin and E. E. Karyakina, *Russ. Chem. Bul.*, International Edition, 50 (2001) 10, 1811-1817.
3. D. Ellis, M. Eckhoff and V. D. Neff, *J. Phys. Chem.*, 85 (1981) 1225-1231.
4. K. Itaya, T. Ataka and S. Toshima, *J. Am. Chem. Soc.*, 104 (1982) 18, 4767-4772.
5. F. Herren, P. Fisher, A. Ludi and W. Haelg, *Inorg. Chem.*, 19 (1980) 4, 956-959.
6. P. J. Kulesza, M. A. Malik, M. Berrettoni, M. Giorgetti, S. Zamponi, R. Schmidt and R. Marassi, *J. Phys. Chem. B*, 102 (1998) 11, 1870-1876.
7. C. M. Pharr and P. R. Griffiths, *Anal. Chem.*, 69 (1997) 22, 4665-4672.
8. H. J. Buser, A. Ludi, W. Petter and D. Schwarzenbach, *Chem. Comm.*, 23 (1972) 1299.
9. M. Verdaguer, N. Galvez, R. Garde and C. Desplanches, *The Electrochem. Soc. Interface.*, (2002) 28-32.
10. J. F. Keggin and F. D. Miles, *Nature*, 137 (1936) 577-578.
11. H. J. Buser, D. Schwarzenbach, W. Petter and A. Ludi, *Inorg. Chem.*, 16 (1977) 11, 2704-2710.
12. R. M. Bozorth, H. J. Williams and D. E. Walsh, *Phys. Rev.*, 103 (1956) 572-578.
13. O. Makowski, J. Stroka, P. Kulesza, M. A. Malik and Z. Galus, *J. of Electroanal. Chem.*, 532 (2002) 1-2, 157-164.
14. P. Zhou, D. Xue, H. Luo and X. Chen, *Nano-Letters*, 2 (2002) 8, 845-847.
15. P. Zhou, D. Xue, H. Luo and H. Shi, *Hyperfine Interactions*, 142 (2002) 601-606.
16. Ch. –L. Lin and K. –Ch. Ho, *J. of Electroanal. Chem.*, 524 – 525 (2002) 286-293.
17. F. Ricci and G. Palleschi, *Biosens. Bioelectron.*, 21 (2005) 3, 389-407.
18. R. J. H. Clark and R. E. Hester, *Advances in Infrared and Raman Spectroscopy*, Wiley Press: New York, NY, USA, Vol. 12 (1985) 25.
19. J. J. García-Jareño, J. Navarro-Laboulais and F. Vicente, *Electrochim. Acta*, 41 (1996) 6, 835-841.
20. J. A. Nóbrega and G. S. Lopes, *Talanta*, (1996) 43, 971-976.
21. D. Moscone, D. D'Ottavi, D. Compagnone, G. Palleschi and A. Amine, *Anal. Chem.*, 73 (2001) 2529-2535.

22. R. Saliba, B. Agricole, Ch. Mingotaud and S. Ravaine, *J. Phys. Chem. B*, 103 (1999) 9712-9716.
23. J. J. García-Jareño, A. Sanmatías, J. Navarro-Laboulais and F. Vicente, *Electrochim. Acta*, 44 (1998) 395-405.
24. R. J. Mortimer and D. R. Rosseinsky, *J. of Electroanal. Chem.*, 151 (1983) 133-147.
25. R. J. Mortimer, D. R. Rosseinsky and A. Glidle, *Sol. Energy Mater. Solar Cells*, 25 (1992) 3-4, 211-223.
26. P. Glatzel, L. Jacquamet, U. Bergmann, F. M. F. De Groot and S. P. Cramer, *Inorg. Chem.*, 41 (2002) 12, 3121-3127.
27. A. Ito, M. Suenaga and K. Ono, *J. of Chem. Phys.*, 48 (1968) 8, 3597-3599.
28. K. Itaya, N. Shoji and I. Uchida, *J. Am. Chem. Soc.*, 106 (1984) 3423-3429.
29. Z. Jin and Sh. Dong, *Electrochim. Acta*, 35 (1990) 1057-1060.
30. K. Itaya, I. Uchida and V. D. Neff, *Acc. Chem. Res.*, 19 (1986) 6, 162-168.
31. Sh. Dong and Z. Jin, *Electrochim. Acta*, 34 (1989) 7, 963-968.
32. P. J. Kulesza, S. Zamponi, M. A. Malik, K. Miecniowski, M. Berrettoni and R. Marassi, *J. Solid State Electrochem.*, 1 (1997) 88-93.
33. F. Scholz and A. Dostal, *Angew. Chem. Int. Ed. Engl.*, 34 (1996) 23, 2685-2687.
34. A. A. Karyakin, E. E. Karyakina and L. Gorton, *Electrochem. Commun.*, 1 (1999) N2, 78-82.
35. A. I. Vogel, *Textbook of Macro and Semimicro Qualitative Inorganic Analysis*, 5th Edition, Longman: London (1979).
36. J. J. Garcia-Jareño, J. J. Navarro, A. F. Roig, H. Scholl and F. Vicente, *Electrochim. Acta*, 40 (1995) 9, 1113-1119.
37. M. Jayalakshmi and F. Scholz, *J. Power Sources*, 91 (2000) 2, 217-223.
38. V. D. Neff, *J. Electrochem. Soc.*, 132 (1985) 1382-1384.
39. M. Kaneko and T. Okada, *J. of Electroanal. Chem.*, 255 (1988) 1-2, 45-52.
40. G. Cheng and Sh. Dong, *Electrochim. Acta*, 32 (1987) 11, 1561-1565.
41. P. J. Kulesza, K. Miecniowski, M. Chojak, M. A. Malik, S. Zamponi, R. Marassi, *Electrochim. Acta*, 46 (2001) 4371-4378.
42. D. Ellis, M. Eckhoff and D. Neff, *J. Phys. Chem.*, 85 (1981) 9, 1225-1231.
43. A. Viehbeck and D. W. DeBerry, *J. Electrochem. Soc.*, 132 (1985) 1369-1375.
44. K. Itaya, K. Shibayama, H. Akahoshi and S. Thoshima, *J. Appl. Phys.*, 53 (1982) 804-805.
45. P. M. S. Monk, R. J. Mortimer and D. R. Rosseinsky, *Electrochromism: Fundamentals and Applications*, VCH: Weinheim, Germany, Chapter 6 (1995).
46. R. J. Mortimer and Ch. P. Warren, *J. of Electroanal. Chem.*, 460 (1999) 263-266.
47. B. P. Jelle and G. Hagen, *J. of Appl. Electrochem.*, 28 (1998) 1061-1065.
48. U. Scharf and E. W. Grabner, *Electrochim. Acta*, 41 (1996) 2, 233-239.
49. T. Abe, F. Taguchi, S. Tokita and M. Kaneko, *J. Mol. Catal. A: Chem.*, 126 (1997) 2-3, L89-L92.
50. K. Ogura and I. Yoshida, *Electrochim. Acta*, 32 (1987) 1191-1195.
51. M. Kaneko, Sh. Hara and A. Yamada, *J. of Electroanal. Chem.*, 194 (1985) 1, 165-168.
52. D. F. Watson, J. L. Willson and A. B. Bocarsly, *Inorg. Chem.*, 41 (2002) 2408-2416.
53. V. Escax, A. Bleuzen, J. P. Itié, P. Munsch, F. Varret and M. Verdaguer, *J. Phys. Chem. B*, 107 (2003) 20, 4763-4767.
54. G. R. Torres, E. Dupart, Ch. Mingotaud and S. Ravaine, *J. Phys. Chem. B*, 104 (2000) 9487-9490.
55. M. Pyrasch and B. Tieke, *Langmuir*, 17 (2001) 7706-7709.
56. W. E. Buschmann and J. S. Miller, *Inorg. Chem.*, 39 (2000) 11, 2411-2421.
57. M. Verdaguer, A. Bleuzen, V. Marvaud, J. Vaissermann, M. Seuleiman, C. Desplanches, A. Sculler, C. Train, R. Garde, G. Gelly, C. Lomenech, I. Rosenman, P. Veillet, C. Cartier and F. Villain, *Coord. Chem. Rev.*, 190 – 192 (1999) 1023-1047.
58. J. T. Culp, J. -H. Park, I. O. Benitez, Y. -D. Huh, M. W. Meisel and D. R. Talham, *Chem. Matter.*, (2003) A-F.
59. C. Mingotaud, C. Lafuente, J. Amiell and P. Delhaes, *Langmuir*, 15 (1999) 2, 289-292.

60. Z. Ding, Ch. Yang and Q. Ch.; Wu, Q. The Electrochemical Generation of Ferrate at Porous Magnetite Electrode, *Electroanalysis*, 2004, 49, 3155-3159.
61. Sh. –I. Ohkoshi and K. Hashimoto, *The Electrochem. Soc. Interface*, (2002) 34-38.
62. R. Garde, F. Villain and M. Verdaguer, *J. Am. Chem. Soc.*, 124 (2002) 35, 10531-10538.
63. G. Rogez, S. Parsons, C. Paulsen, V. Villar and T. Mallanh, *Inorg. Chem.*, 40 (2001) 16, 3836-3837.
64. N. Shimamoto, Sh. –I. Ohkoshi, O. Sato, and K. Hashimoto, *Inorg. Chem.*, 41 (2002) 4, 678-684.
65. A. Bleuzen, C. Lomenech, V. Escax, F. Villain, F. Varret, Ch. Cartier dit Moulin and M. Verdaguer, *J. Am. Chem. Soc.*, 122 (2000) 6648-6652.
66. Sh. Chen, R. Yuan, Y. Chai, Y. Xu, L. Min and N. Li, *Sens. and Act. B*, 135 (2008) 1, 236-244.
67. H. Kahlert, U. Retter, H. Lohse, K. Siegler and F. Scholz, *J. Phys. Chem. B*, 102 (1998) 8757-8765.
68. O. Chaofeng, Ch. Shihong, Y. Ruo, Ch. Yaqin and Z. Xia, *J. of Electroanal. Chem.*, 624 (2008) 1-2, 287-292.
69. V. Vo, N. V. Minh, H. I. Lee, J. M. Kim, Y. Kim and S. J. Kim, *Mat. Res. Bull.*, 44 (2009) 8, 78-81.
70. F. Li and Sh. Dong, *Electrochim. Acta*, 32 (1987) 1511-1513.
71. A.A. Karyakin, *Electroanalysis*, 13 (2001) 10, 813-819.
72. A.A. Karyakin, E. E. Karyakin and L. Gorton, *Anal. Chem.*, 72 (2000) 1720-1723.
73. A.A. Karyakin, E. A. Kotel'nikova, L. V. Lukachova, E. E. Karyakin and J. Wang, *Anal. Chem.*, 74 (2002) 1597-1603.
74. E. Katz and I. Willner, *Angew. Chem. Int. Ed.*, 43 (2004) 6042-6108.
75. K. Derwinska, K. Miecniowski, R. Koncki, P. J. Kulesza, S. Glab and M. A. Malik, *Electroanalysis*, 15 (2003) 23-24, 1843-1849.
76. M. R. Deakin and H. Byrd, *Anal. Chem.*, 61 (1989) 4, 290-295.
77. T. J. Ikeshoji, *Electrochem. Soc.*, 133 (1986) 2108-2109.
78. G. Zhiqiang, Z. Xiangyao, W. Guangqing, L. Peibiao and Z. Zaofan, *Anal. Chimica Acta*, 244 (1991) 39-48.
79. L. Li, Q. Sheng, J. Zheng and H. Zhang, *Bioelectrochemistry*, 74 (2008) 1, 170-175.
80. N. A. Pchelintsev, F. Neville and P. A. Millner, *Sens. and Act. B: Chem.*, 135 (2008) 1, 21-26.
81. J. A. Cox and B. K. Das, *Anal. Chem.*, 57 (1985) 13, 2739-2740.
82. V. Krishnan, A. L. Xidis and V. D. Neff, *Anal. Chim. Acta.*, 239 (1990) 7-12.
83. A. K. Jain, R. P. Singh and Ch. Bala, *J. Chem. Technol. & Biotechnol.*, 34 (1984) 7, 363-366.
84. K. N. Thomsen and R. P. Baldwin, *Anal. Chem.*, 61 (1989) 23, 2594-2598.
85. K. N. Thomsen and R. P. Baldwin, *Electroanalysis*, 2 (1990) 4, 263-271.
86. Y. Tani, H. Eun and Y. A. Umezawa, *Electrochim. Acta*, 43 (1998) 23, 3431-3441.
87. U. Scharf and E. W. Grabner, *Electrochim. Acta*, 41 (1996) 2, 233-239.
88. A.A. Karyakin, O. V. Gitelmacher and E. E. Karyakina, *Anal. Chem.*, 67 (1995) 14, 2419-2423.
89. J. Zhu, Z. Zhu, Z. Lai, R. Wang, X. Guo, X. Wu, G. Zhang, Z. Zhang, Y. Wang and Z. Chen, *Sensors*, 2 (2002) 127-136.
90. D. Zhang, K. Zhang, Y. L. Yao, X. H. Xia and H. Y. Chen, *Langmuir*, 20 (2004) 7303-7307.
91. A.P. Xagas, M. C. Bernard, A. G. Hugot-Le, N. Spyrellis, Z. Loizos and P. Falaras, *J. Of Photochem. and Photob. A: Chem.*, 132 (2000) 115-120.
92. G. G. Gulbault and G. Lubrano, *J. Anal. Chim. Acta*, 64 (1973) 3, 439-455.
93. J. –M. Zen, P. –Y. Chen and A. S. Kumar, *Anal. Chem.*, 75 (2003) 21, 6017-6022.
94. M. F. De Oliveira, A. A. Saczk, J. A. Gomes, P. S. Roldan and N. R. Stradiotto, *Sensors*, 3 (2003) 371-380.
95. G. R. Newkome, C. N. Moorefield and F. Vögtle, *Dendritic Molecules: Concepts, Syntheses and Perspectives*, VCH: Weinheim, Germany (1996).

96. R. M. Crooks, B. I. Lemon, L. Sun, L. K. Yeung and M. Zhao, *Dendrimers: Design, Dimension and Function*, Springer – Verlag: Berlín (2001).
97. D. A. Tomalia, S. Uppuluri, D. R. Swanson and J. Li, *Pure Appl. Chem.*, 12 (2000) 2343-2358.
98. K. M. A. Rahman, C. J. Durning, N. J. Turro and D. A. Tomalia, *Langmuir*, 16 (2000) 26, 10154-10160.
99. F. N. Crespilho, V. Zucolotto, Ch. M. A. Brett, O. N. Oliveira and F. C. Nart, *J. Phys. Chem. B*, 110 (2006) 35, 17478-17483.
100. L. Balogh and D. A. Tomalia, *J. Am. Chem. Soc.*, 120 (1998) 29, 7355-7356.
101. Y. Zhou, M. L. Bruening, D. E. Bergbreiter, R. M. Crooks and M. Wells, *J. Am. Chem. Soc.*, 118 (1996) 3773 – 3774.
102. J. F. G. A. Jansen, E. W. Meijer and –V. E. M. M. De Be Den Berg, *J. Am. Chem. Soc.*, 117 (1995) 15, 4417-4418.
103. S. C. Zimmerman, M. S. Wendland, N. A. Rakow, I. Zharov and K. S. Suslick, *Nature*, 418 (2002) 399-403.
104. A. Archut, G. C. Azzellini, V. Balzani, L. De Cola and F. Vögtle, *F. J. Am. Chem. Soc.*, 120 (1998) 47, 12187-12191.
105. V. Chechik and R. M. Crooks, *J. Am. Chem. Soc.*, 122 (2000) 6, 1243-1244.
106. L. K. Yeung and R. M. Crooks, *Nano Lett.*, 1 (2001) 14-17.
107. E. Bustos, J. Manríquez, G. Orozco and L. A. Godínez, *Langmuir*, 21 (2005) 3013-3021.
108. E. Bustos, Th. W. Chapman, R. Rodríguez-Valadez and L. A. Godínez, *Electroanalysis*, 18 (2006) 21, 2092-2098.
109. E. Bustos, M. G. García, E. Juaristi, Th. W. Chapman and L. A. Godínez, *ECS Transactions: Electrochemistry of Supramolecular and Fullerenes Systems*, 3 (2006) 12, 45-57.
110. R. W. J. Scott, O. M. Wilson and R. M. Crooks, *J. Phys. Chem. B*, 109 (2005) 2, 692-704.
111. R. M. Crooks and M. Zhao, *Adv. Mater.*, 11 (1999) 3, 217-220.
112. S. –K. Oh, Y. –G. Kim, H. Ye and R. M. Crooks, *Langmuir*, 19 (2003) 24, 10420-10425.
113. H. Ye, R. W. Scott and R. M. Crooks, *Langmuir*, 20 (2004) 7, 2915-2920.
114. K. Esumi, R. Nakamura, A. Suzuki and K. Torigoe, *Langmuir*, 16 (2000) 20, 7842-7846.
115. Y. Li, A. Mostafa and J. El-Sayed *J. of Phys. Chem. B*, 105 (2001) 37, 8938-8943.
116. M. Ooe, M. Murata, T. Mizugaki, K. Eitani and K. Kaneda, *Nano Lett.*, 2 (2002) 9, 999-1000.
117. Y. –G. Kim, S. –K. Oh and R. M. Crooks, *Chem. Mater.*, 16 (2004) 1, 167-172.
118. F. Gröhn, B. J. Bauer, Y. A. Akpalu, C. L. Jackson and E. J. Amis, *Macromolecules*, 33 (2000) 16, 6042-6050.
119. F. Gröhn, X. Gu, H. Grüll, J. C. Meredith, G. Nisato, B. Bauer, A. Karim and E. J. Amis, *Macromolecules*, 35 (2002) 13, 4852-4854.
120. K. Esumi, K. Satoh and K. Torigoe, *Langmuir*, 2001, 17, 22, 6860-6864.
121. M. Zhao, L. Sun and R. M. Crooks, *J. Am. Chem. Soc.*, 120 (1998) 19, 4877-4878.
122. R. W. J. Scott, A. K. Datye and R. M. Crooks, *J. Am. Chem. Soc.*, 125 (2003) 13, 3708-3709.
123. R. W. J. Scott, O. M. Wilson, S. –K. Oh, E. A. Kenik and R. M. Crooks, *J. Am. Chem. Soc.*, 126 (2004) 47, 15583-15591.
124. O. M. Wilson, R. W. J. Scott, J. C. García-Mantínez and R. M. Crooks, *J. Am. Chem. Soc.*, 127 (2005) 3, 1015-1024.
125. K. Esumi, T. Hosoya, A. Suzuki and K. Torigoe, *Langmuir*, 16 (2000) 6, 2978-2980.
126. Y. –G. Kim, S. –K. Oh and R. M. Crooks, *Chem. Mater.*, 2004, 16, 167.
127. B. M. Quinn, P. Liljeroth, V. Ruiz, T. Laaksonen and K. Kontturi, *J. Am. Chem. Soc.*, 125 (2003) 22, 6644-6645.
128. R. Kötz and M. Carlen, *Electrochim. Acta*, 45 (2000) 15-16, 2483-2498.
129. T. R. Jensen, M. D. Malinsky, C. L. Haynes and R. P. Van Duyne, *J. Phys. Chem. B.*, 104 (2000) 45, 10549-10556.

130. N. A. Pchelintsev, A. Vakurov and P. A. Millner, *Sens. and Act. B: Chem.*, 138 (2009) 2, 461-466.
131. Y. Guo, A. R. Guadalupe, O. Resto, L. F. Fonseca and S. Z. Weisz, *Chem. Mater.*, 11 (1999) 1, 135-140.
132. M. Giorgetti, M. Berrettoni, S. Zamponi, P. J. Kulesza and J. A. Cox, *Electrochim. Acta*, 51 (2005) 511-516.
133. J. Lurie, *Handbook of Analytical Chemistry*, Mir Publishers: Moscow (1975).
134. S. A. Jaffari and A. P. F. Turner, *Biosens. Bioelectron.*, 12 (1997) 1, 1-7.
135. N. B. Li, J. H. Park, K. Park, S. J. Kwon, H. Shin and J. Kwak, *Biosens. Bioelectron.*, 23 (2008) 10, 1519-1526.
136. C. Gabrielli, J. J. García-Jareño, M. Keddam, H. Perrot and F. Vicente, *J. Phys. Chem. B*, 106 (2002) 12, 3182-3191.
137. A. Abbaspour and M. A. Kamyabi, *J. of Electroanal. Chem.*, 584 (2005) 117-123.
138. V. M. Ivama and S. H. P. Serrano, *J. Braz. Chem. Soc.*, 14 (2003) 4, 551-555.
139. U. Schröder and F. Scholz, *Inorg. Chem.*, 39 (2000) 5, 1006-1015.
140. T. J. O'Shea, M. W. Telting-Díaz, S. M. Lunte, C. E. Lunte and M. R. Smyth, *Electroanalysis*, 4 (1992) 4, 463-468.
141. S. Zamponi, M. Giorgetti, M. Berrettoni, P. J. Kulesza, J. A. Cox and A. M. Kijak, *Electrochimica Acta*, 51 (2005) 118 – 124.
142. M. Giorgetti, M. Berrettoni, S. Zamponi, P. J. Kulesza and J. A. Cox, *Electrochim. Acta*, 51 (2005) 3, 511-516.
143. R. W. J. Scott, A. K. Datye and R. M. Crooks, *J. Am. Chem. Soc.*, 125 (2003) 13, 3708-3709.
144. H. Ye and R. M. Crooks, *J. Am. Chem. Soc.*, 127 (2005) 13, 4930-4934.
145. R. Crooks, M. B. I. Lemon III, L. Sun, L. K. Yeung and M. Zhang, *Dendrimer-Encapsulated Metals and Semiconductors: Synthesis, Characterization and Applications*, Springer: New York, USA (2001).
146. A.A. Karyakin, E. E. Karyakina and L. Gorton, *Talanta*, 43 (1996) 1597-1606.
147. A.A. Karyakin, E. E. Karyakina and L. Gorton, *J. Electroanal. Chem.*, 456 (1998) 97-104.
148. Sh. Wu, T. Wang, Ch. Wang, Z. Gao and Ch. Wang, *Electroanalysis*, 19 (2007) 6, 659-667.
149. E. Bustos, M. G. García, B. R. Díaz-Sánchez, E. Juaristi and L. A. Godínez, *Talanta*, 72 (2007) 1586-1592.
150. H. Kahlert, U. Retter, H. Lohse, K. Siegler and F. Scholz, *J. Phys. Chem. B*, 102 (1998) 44, 8757-8765.
151. Y. Liu, Z. Chu and W. Jin, *Electrochem. Commun.*, 11 (2009) 2, 484-487.
152. A. Abbaspour and M. A. Kamyabi, *J. of Electroanal. Chem.* 584 (2005) 2, 117-123.
153. M. Orellana, P. Arriola, R. Del Río, R. Schrebler, R. Cordova, F. Scholz and H. Kahlert, *J. Phys. Chem. B*, 109 (2005) 15483-15488.
154. L. J. Curtman, *Análisis Químico Cualitativo: Basado en las Leyes de Equilibrio y en la Teoría de la Ionización*. Editora Nacional México: México City (1963) 221.
155. G. Svehla, *Vogel's Qualitative Inorganic Analysis*, 6th Edition, Longman Group: Essex, U. K. (1987) 169.
156. H. Tokuhisa, M. Zhao, L. A. Baker, V. T. Phon, D. L. Dermody, M. E. García, M. E.; R. F. Peez, R. M. Crooks and Th. M. Mayer, *J. Am. Chem. Soc.*, 120 (1998) 18, 4492-4501.
157. J. Manríquez, E. Juaristi, O. Muñoz – Muñiz and L. A. Godínez, *Langmuir*, 19 (2003) 18, 7315-7323.
158. D. Giménez-Romero, P. R. Bueno, C. Castaño, C. Gabrielli, H. Perrot, J. J. García – Jareño and F. Vicente, *Electrochem. Commun.*, 8 (2006) 371-374.
159. J. Drexler and C. Steimen, *J. Phys. Chem. B*, 107 (2003) 40, 11245-11254.
160. O. E. Barcia, E. D'Elia, I. Frateru, O. R. Mattos, N. Pébere and B. Tribollet, *Electrochim. Acta*, 47 (2002) 13-14, 2109-2116.

161. H. Kahlert, U. Retter, H. Lohse, K. Siegler and F. Scholz, *J. Phys. Chem. B*, 102 (1998) 8757-8765.
162. D. A. Buttry, *Applications of the quartz crystal microbalance to electrochemistry*, Bard, J. Ed. Marcel Dekker: New York, USA, Vol. 17 (1991) 1.
163. A. Olivier, J. P. Chopart, J. Douglade, C. Gabrielli and B. Tribollet, *J. of Electroanal. Chem.*, 1-2 (1987) 275-279.
164. B. J. Feldman and O. R. Melroy, *J. of Electroanal. Chem.*, 234 (1987) 1-2, 213-227.
165. E. Czirók, J. Bácskai, P. J. Kulesza, G. Inzelt, A. Wolkiewicz, K. Miecznikowski and M. A. Malik, *J. of Electroanal. Chem.*, 405 (1996) 1-2, 205-209.
166. M. A. Malik, K. Miecznikowski and P. J. Kulesza, *Electrochim. Acta*, 45 (2000) 22-23, 3777-3784.
167. S. J. Lasky and D. A. Buttry, *J. Am. Chem. Soc.*, 110 (1988) 18, 6258-6260.
168. Southampton Electrochemistry Group, *Instrumental Methods in Electrochemistry*, Horwood, New York, Chapter 8 (1993).
169. J. R. Macdonald, *Impedance Spectroscopy*, Wiley: New York, USA (1987).
170. M. M. Musiani, *Electrochim. Acta*, 35 (1990) 10, 1665-1670.
171. I. Oh, H. Lee, H. Yang and J. Kwak, *Electrochem. Commun.*, 3 (2001) 274 – 280.
172. R. Garde, F. Villain and M. Verdager, *J. Am. Chem. Soc.*, 124 (2002) 35, 10531-10538.
173. P. A. Christensen, A. Hamnett and P. R. Trevellick, *J. of Electroanal. Chem.*, 242 (1988) 23-45.
174. J. M. Chalmers and P. R. Griffiths, *Handbook of Vibrational Spectroscopy: Applications in Industry, Materials and the Physical Science*. Ed. John Wiley & Sons, Ltd.: West Sussex, U.K. Vol. 3 (2002) 1791-1794.
175. J. M. Chalmers and P. R. Griffiths, *Handbook of Vibrational Spectroscopy: Applications in Industry, Materials and the Physical Science*. Ed. John Wiley & Sons, Ltd.: West Sussex, U.K. Vol. 4 (2002) 2915.
176. J. Lipkowski and Ph. N. Ross, *Adsorption of Molecules at Metal Electrodes*, VCH: New York (1992) 318.
177. S. Zamponi, A. M. Kijak, A. J. Sommer, R. Marassi, P. J. Kulesza and J. A. Cox, *J. Solid State Electrochem.*, 6 (2002) 528-533.
178. R. W. J. Scott, O. M. Wilson and R. M. Crooks, *J. Phys. Chem. B*, 109 (2005) 2, 692-704.
179. P. J. Kulesza, S. Zamponi, M. Berrettoni, R. Marassi and M. A. Malik, *Electrochim. Acta*, 40 (1995) 6, 681-688.
180. M. Kaneko and T. Okada, *J. of Electroanal. Chem.*, 255 (1988) 1-2, 45-52.
181. S. J. Lasky and D. A. Buttry, *J. Am. Chem. Soc.*, 110 (1988) 18, 6258-6260.
182. M. R. Deakin and H. Byrd, *Anal. Chem.*, 61 (1989) 4, 290-295.
183. B. D. Humphrey, S. Sinha and A. B. Bocarsly, *J. Phys. Chem.*, 91 (1987) 3, 586-593.
184. Sh. -M. Chen, *Electrochim. Acta*, 43 (1998) 21-22, 3359-3369.
185. A.A. Karyakin, E. E. Karyakina and L. Gordon, *Electrochem. Commun.*, 1 (1999) 78-82.
186. J. Zhou and E. Wang, *J. of Electroanal. Chem.*, 331 (1992) 1-2, 1029-2043.
187. K. Ogura and I. Yoshida, *Electrochim. Acta*, 8 (1987) 32, 1191-1195.
188. K. Honda and H. Hayashi, *J. Electrochem. Soc.*, 134 (1987) 1330-1334.
189. P. M. S. Monk, R. J. Mortimer and D. R. Rosseinsky, *Electrochromism, fundamentals and applications*, VCH: Weinheim, Chapter 6 (1995).
190. H. Kellawi and D. R. Rosseinsky, *J. of Electroanal. Chem.*, 131 (1982) 8, 373-376.
191. E. A. R. Duek, M. -A. De Paoli and M. Mastragostino, *Adv. Mater.*, 5 (1993) 9, 650-652.
192. M. Jayalaxmi and F. Scholz, *J. Power Sources*, 91 (2000) 2, 217-223.
193. N. Imanish, T. Morikawa, K. Kondo, Y. Takeda, O. Yamamoto, N. Kinugasa and T. Yamagishi, *J. Power Sources*, 79 (1999) 2, 215-219.
194. Sato, O.; Einaga, Y.; Iyoda, T.; Fujishima, A.; Hashimoto, K. *J. Phys. Chem. B.*, 101 (1997) 20, 3903-3905.

195. S. S. Kumar, J. Mathiyarasu and K. L. Phani, *J. of Electroanal. Chem.*, 578 (2005) 1, 95-103.
196. S. S. L. Castro, V. R. Balbo, P. J. S. Barbeira and N. R. Stradiotto, *Talanta*, 55 (2001) 249-254.
197. T. Selvaraju and R. Ramaraj, *Electrochem. Commun.*, 5 (2003) 667-672.
198. M. B. Davies, J. Austin and D. A. Partridge, *Vitamin C. In Chemistry and Biochemistry*, The Royal Society of Chemistry, Cambridge (1991).
199. A.A. Karyakin, E. A. Puganova, I. A. Budashov, I. N. Kurochkin, E. E. Karyakina, V. A. Levchenko, V. N. Matveyenko and S. D. Varfolomeyev, *Anal. Chem.*, 76 (2004) 474-478.
200. I.F. Cheng, F. Quintus and N. Korte, *Environ. Sci. Technol.*, 31 (1997) 4, 1074-1078.
201. F. Zeng and S. C. Zimmerman, *Chem. Rev.*, 97 (1997) 1681-1712.
202. K. Kago, H. Matsuoka, R. Yoshitome, E. Mouri and H. Yamaoka, *Langmuir*, 15 (1999) 12, 4295-4301.
203. N. Priyantha and D. Weerabahu, *Anal. Chim. Acta*, 320 (1996) 2-3, 263-268.
204. G. R. Newkome, C. N. Moorefield and F. Vögtle, *Dendritic Molecules: Concepts, Syntheses and Perspectives*, VCH: Weinheim, Germany (1996).
205. R. M. Crooks, M. Zhao, L. Sun, V. Chechik and L. K. Yeung, *Acc. Chem. Res.*, 34 (2001) 3, 181-190.
206. H. Lund and M. M. Baizer, *Organic Electrochemistry: An Introduction and a Guide*, 3rd Edition, Marcel Dekker: New York, USA (1991) 645.
207. C. G. Tsiafoulis, P. N. Trikalitis and M. I. Prodromidis, *Electrochem. Commun.*, 7 (2005) 12, 1398-1404.
208. Y. Wang, J. Huang, Ch. Zhang, J. Wei and X. Zhou, *Electroanalysis*, 10 (1998) 11, 776-778.
209. W. B. Nowall and W. G. Kuhr, *Electroanalysis*, 9 (1997) 2, 102-109.
210. N. B. Li, J. H. Park, K. Park, S. J. Kwon, H. Shin and J. Kwak, *Biosens. Bioelectron.*, 23 (2008) 10, 1519-1526.
211. F. Ricci and G. Palleschi, *Biosens. Bioelectron.*, 21 (2005) 3, 389-407.
212. A.A. Karyakin, O. V. Gitelmacher and E. E. Karyakina, *Anal. Chem.*, 67 (1995) 2419-2423.
213. A.A. Karyakin and E. E. Karyakina, *Sens. Actuators, B.*, 57 (1999) 1-3, 268-273.
214. V. M. Jovanovic, S. Terzic, A. V. Tripkovic, K. Dj. Popovic and J. D. Lovic, *Electrochem. Commun.*, 6 (2004) 12, 1254-1258.
215. Ch. -L. Lin and K. -Ch. Ho, *J. of Electroanal. Chem.*, 524 – 525 (2002) 286-293.
216. B. E. Conway, *Ionic Hydration in Chemistry and Biophysics: Studies in Physical and Theoretical Chemistry*, Elsevier: Amsterdam (1981) 73.
217. Y. Zhang and G. S. Wilson, *J. of Electroanal. Chem.*, 345 (1993) 1-2, 253-271.